HAL open science

Dynamic contributions of stratified groundwater to streams controls seasonal variations of streamwater transit times

Jean Marçais, Louis A Derry, Luca Guillaumot, Luc Aquilina, Jean-Raynald de Dreuzy

To cite this version:

Jean Marçais, Louis A Derry, Luca Guillaumot, Luc Aquilina, Jean-Raynald de Dreuzy. Dynamic contributions of stratified groundwater to streams controls seasonal variations of streamwater transit times. Water Resources Research, In press, pp.e2021WR029659. 10.1029/2021wr029659 . insu-03579375v1

HAL Id: insu-03579375

https://insu.hal.science/insu-03579375v1

Submitted on 18 Feb 2022 (v1), last revised 30 Mar 2022 (v2)

HAL is a multi-disciplinary open access archive for the deposit and dissemination of scientific research documents, whether they are published or not. The documents may come from teaching and research institutions in France or abroad, or from public or private research centers.

L'archive ouverte pluridisciplinaire **HAL**, est destinée au dépôt et à la diffusion de documents scientifiques de niveau recherche, publiés ou non, émanant des établissements d'enseignement et de recherche français ou étrangers, des laboratoires publics ou privés.

Check for updates

Dynamic contributions of stratified groundwater to streams controls seasonal variations of streamwater transit times

Jean Marçais[1,2], Louis A. Derry [3,2], Luca Guillaumot[4,5], Luc Aquilina[4], Jean-Raynald de Dreuzy [4,6]

[1]INRAE, UR Riverly, F-69625 Villeurbanne, France
[2]Institut de Physique du Globe de Paris, Université de Paris, CNRS, F-75005 Paris, France
[3]Department of Earth and Atmospheric Sciences, Cornell University, Ithaca, NY
[4]Univ Rennes, CNRS, Géosciences Rennes - UMR 6118, F-35000 Rennes, France
[5]International Institute for Applied Systems Analysis, Laxenburg, Austria
[6]Univ Rennes, CNRS, OSUR Observatoire des sciences de l'univers de Rennes - UMS 3343, F-35000 Rennes, France

Key Points:

- Hydraulic conductivity controls groundwater flow contributions to streams while porosity directly scales the streamwater mean transit times.
- Seasonal groundwater contributions to streams modulate the mean transit times dynamics from 6 years at high flows to 20 years at low flows.
- Stratified groundwater ages lead to a significant fraction (> 75 %) of old water to streamflow (>1 year).

Corresponding author: Jean Marçais, `jean.marcais@inrae.fr`

This article has been accepted for publication and undergone full peer review but has not been through the copyediting, typesetting, pagination and proofreading process, which may lead to differences between this version and the Version of Record. Please cite this article as doi: 10.1029/2021WR029659.

This article is protected by copyright. All rights reserved.

Accepted Article

Abstract

Streamwater transit time distributions display a variable proportion of old waters (≥1 yr). We hypothesize that the corresponding long transit times result from groundwater contributions to the stream and that seasonal streamwater transit time variations result from 1) the variable contributions of different flowpaths (overland flow, seepage flow and baseflow) and 2) the stratification of groundwater residence times. We develop a parsimonious model to capture the groundwater contribution to the stream discharge and its effect on transient transit times. Infiltration is partitioned according to the aquifer saturation between Boussinesq groundwater flow and overland flow. Time-variable transit time distributions are obtained with a new 2D particle tracking algorithm. Hydraulic conductivity, total and drainable porosities are calibrated by using discharge and CFC tracer data on a crystalline catchment located in Brittany (France). The calibrated models succeed in reproducing CFCs concentrations and discharge dynamics. The groundwater flow contribution to the stream is controlled by the aquifer hydraulic conductivity, while its age is controlled by the drainable and total porosities. Old groundwater (≥1 yr) is the source for approximately 75 % of the streamflow with strong seasonal variations (between 40 and 95 %). Mean transit times are approximately 13 years, varying between 6 and 20 years, inversely proportional to the groundwater contribution. These seasonal variations are driven by the groundwater versus overland flow partitioning. The stratification of groundwater residence times in the aquifer plays a minor role in the streamwater transit times but is key for the transit time dynamics of the groundwater contribution to the stream.

Plain Language Summary

Water entering a catchment as precipitation can take multiple paths with different transit times to the stream. While a significant fraction of water has short transit times (i.e. is "young") when it reaches the stream, there is also an important contribution of "old" water with long transit times in the subsurface. The age distribution of this old component is important for understanding the resilience of watersheds to climate change, the behavior of persistent pollutants and chemical weathering processes. We developed a model, informed with discharge time series and atmospheric age tracer (CFCs), to constrain the age distribution in both groundwater and streamwater and how they vary seasonally. In our temperate test catchment with crystalline bedrock (Brittany, France), we find that the mean age of streamwater exiting the catchment is approximately 13 years, but varies seasonally from 6 to 20 years as the relative contributions of older groundwater and younger runoff change. Groundwater stratification further influences the mean age of the groundwater contribution arriving at the stream.

1 Introduction

Transit time is the time elapsed between the moment a water molecule enters a hydrological system (e.g. a catchment) and the moment it exits (e.g. through discharge) (Sprenger et al., 2019). This quantity is a fundamental descriptor of the hydrological fluxes and transport within the Critical Zone (Botter et al., 2020). Sampled streamwater, comprised of many water molecules with different transit times, reflects the diversity of flowpaths to the stream and its age distribution can provide information about Critical Zone structures (Kirchner et al., 2000, 2001; Brantley et al., 2017; Kuppel et al., 2020). This

This article is protected by copyright. All rights reserved.

Accepted Article

distribution of transit times, though not directly observable, is a powerful integral quantity for understanding catchment-scale processes (Ameli et al., 2017; Gabrielli et al., 2018; Heidbüchel et al., 2020). It varies at different time scales, from the event to the seasonal and interannual time scales, reflecting the interplay between climatic variations and catchment structures as well as their impact on water resources at the catchment scale (Heidbüchel et al., 2013; Remondi et al., 2018, 2019). Characterizing streamwater transit time distributions (TTDs) is therefore critical to define sustainable water use (Ferguson et al., 2020), evaluate climate change impacts on water resources (Maxwell et al., 2016; Fang et al., 2019), assess the effect of contaminant legacy (e.g. agricultural nutrient and pesticides) (van der Velde et al., 2010; Van Meter et al., 2016, 2018; Ehrhardt et al., 2019), as well as better understand Critical Zone evolution through weathering and erosion (Maher, 2010; Maher & Druhan, 2014; Li et al., 2017; R. S. Anderson et al., 2019).

While the distribution of transit times is weighted toward young ages ($\leq$ 1 year) in most catchments (Jasechko et al., 2016; Benettin, Bailey, et al., 2017; Harman, 2014), it also includes a variable and difficult-to-constrain contribution from older water ($\geq$ 1 year) investigated by only few studies (Stolp et al., 2010; Kaandorp et al., 2018; Visser et al., 2019). This old water fraction that has experienced a long transit time in the hydrologic system may be a smaller component of stream fluxes (Gardner et al., 2011), but is critical to constrain for several reasons. These include but are not limited to the following. 1) The resilience of surface water fluxes in the face of climate variability (drought, climate change) can depend heavily on the availability of old groundwater contributions to streamflow (Manning et al., 2012; Solder et al., 2016). 2) The recovery time scale of a watershed with persistent chemical pollutants can be alleviated by the old water contribution due to dilution or reactive processes (Aquilina et al., 2012; Pinay et al., 2015; Van Meter & Basu, 2017; Kolbe et al., 2019). 3) Chemical weathering (water-rock or water-regolith) reactions are often kinetically limited and water components with long reaction time scales are necessary to produce quasi-equilibrium solute and tracer compositions (Maher, 2011; Fernandez et al., 2021). Thus "older" water may be a smaller contributor to stream discharge but can have a disproportionate influence on weathering reactions and streamwater quality (Frisbee et al., 2013). Predicting the future response of watersheds to anthropogenic climate forcing requires that we have an improved ability to accurately model the old component of the distribution of watershed transit times and how that distribution varies in response to hydrologic and landscape forcing (Heidbüchel et al., 2012; Wilusz et al., 2017).

Here we focus on characterizing old streamwater ages ($\geq$ 1 year). We hypothesize that :

- old streamwater transit times result from the high contributions of subsurface aquifers and from strong groundwater flow residence time stratification (i.e. young ages at the top of the aquifer and old ages at the bottom, see Figure 1), tied to the hydraulic properties of the aquifer (porosity, hydraulic conductivity);
- the dynamic partitioning of discharge between groundwater flows and overland flows explains the high seasonal variability of river discharge while the old component of the streamwater does not evolve much.

To assess the relevance of these two processes (i.e. stratification and partitioning) for old mean streamwater transit times and their seasonal variability, we could not use

This article is protected by copyright. All rights reserved.

Accepted Article

previously developed families of transit time models. The first family of models spans all the lumped representation of transit time distribution, from the simple lumped parameters models (Małoszewski & Zuber, 1982; Marçais et al., 2015) to more advanced storage selection function approaches (Harman, 2014; Rinaldo et al., 2015; Benettin, Soulsby, et al., 2017; Benettin & Bertuzzo, 2018; Nguyen et al., 2021). This type of models are not appropriate here because they do not account for spatially explicit processes, which limit their ability to investigate the controls regarding transit time distributions shapes (Gauvain et al., 2021), as well as the impact of different flowpaths contributions to streams on the development of transit time distributions. The second family of models encompasses detailed, spatially explicit process-based models such as Fatichi et al. (2016); X. Yang et al. (2018); Therrien and Sudicky (1996); Kollet and Maxwell (2006); Camporese et al. (2010). Their explicit description requires constraints on a number of parameters that can be difficult to obtain in many circumstances, and whose calibration may not be unique. Besides, due to their high computation requirements, systematic exploration of the variability of response of these models depending on different parameters sets and on main processes represented are often not carried out (Putti & Paniconi, 2004; Paniconi & Putti, 2015). We therefore develop a novel intermediate model that represents what we hypothesize are the key processes playing a first order role for characterizing old streamwater ages and the proportion of old groundwater in streams.

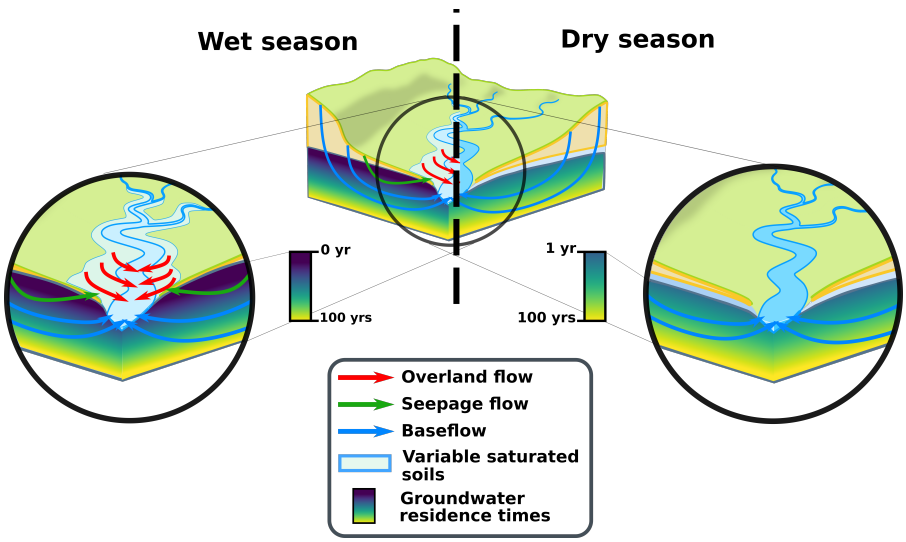

Figure 1. Sketch of the investigated processes. Where the water table intersects the land surface, it generates seepage flow (green arrows) and creates variable saturated areas that are responsive to precipitation (overland flow, red arrows). In the aquifer, groundwater flow is modeled with a Boussinesq formulation (blue arrows) adapted to take into account the groundwater residence time stratification (materialized by the colormap in the aquifer). Note the reduction of overland and seepage flows (red and green arrows) as well as the flush of young groundwater residence times from the wet (left side of the panel) to the dry season (right side of the panel) due to the small displacement of the water table.

We use a semi-explicit hillslope-scale approach that represents groundwater flows inputs to streamwater with the vertically integrated approach proposed by Boussinesq (Boussinesq, 1877; Dupuit, 1863). We modified the Boussinesq model to take into ac-

This article is protected by copyright. All rights reserved.

Accepted Article

count the dynamic partitioning with the saturation excess overland flow and its fast routing to the stream network (S. P. Anderson et al., 1997; Freer et al., 2002; Blume & van Meerveld, 2015). We assume that the partitioning between groundwater flow and overland flow is controlled by the existence of seepage areas when the water table intersects the land surface (section 2.1, Marçais et al. (2017)). To represent the effect of the groundwater residence time stratification (Vogel, 1967; Kolbe et al., 2020), we develop a new transient and stratified transport model (section 2.2) adapted to the hillslope Boussinesq equations (Troch et al., 2003). Further, to overcome classic tracer resolution bias towards the young ages (Kirchner, 2016; Sprenger et al., 2019), we used CFC groundwater age data conjointly with monthly discharge time series to both quantify the groundwater contribution to stream and the transit time distribution dynamics (section 2.3). We test this approach on the 43 km^2 Guillec catchment of Brittany (France) as an example of shallow aquifers in crystalline regions (section 3). We discuss the relevance of such stratification and partitioning processes, the representativity of the calibrated catchment-scale parameters (hydraulic conductivity, drainable and total porosities), and the potential interest and limitations of the approach (section 4).

2 Flow model, transport model and study site

We recall the flux formalism relative to the hillslope storage Boussinesq equation modified to include overland flow generation (Marçais et al., 2017) (Figure 1). Advective transport is represented within a Lagrangian framework and solved with a particle tracking method accounting for the stratification of the solute transport in the aquifer and the routing of the saturation excess overland flow. It allows tracking of particle transit times and travel distances. Dispersive transport is added within the flow lines with an inverse Gaussian distribution. The model computes estimates of time-varying streamflows, transit time distributions of streamwater and residence time distributions of groundwater (Marçais, 2021) and these are compared to flow and transport data of the Guillec catchment (Brittany, France).

2.1 Flow model: partitioning groundwater from overland flow

Groundwater flows are based on a Boussinesq formalism for unconfined shallow aquifers (Troch et al., 2003; Paniconi et al., 2003) modified to account for saturation excess overland flow generation (Marçais et al., 2017). For a hillslope described by the width function ω, the slope of the hillslope bedrock θ, the aquifer thickness d and its hydraulic parameters, the drainable porosity ϕ_d and the hydraulic conductivity k (Figure 2.A), groundwater flows draining to a stream are modeled by:

$$\left\{\begin{array}{rcl} \dfrac{\partial S}{\partial t}(x,t) + q_S(x,t) & = & -\dfrac{\partial Q}{\partial x}(x,t) + N(t)\,\omega(x) \\ q_S(x,t) & = & \mathscr{G}\left(\frac{S(x,t)}{S_c(x)}\right)\mathscr{R}\left(-\dfrac{\partial Q}{\partial x}(x,t) + N(t)\,\omega(x)\right) \\ Q(x,t) & = & -\dfrac{kS(x,t)}{\phi_d}\left(\cos\theta\ \dfrac{\partial}{\partial x}\left(\dfrac{S}{\phi_d\, w}\right)(x,t) + \sin\theta\right) \\ S(x,t) & = & \phi_d\,\omega(x)h(x,t) \\ 0 \ \leq \ S(x,t) & \leq & S_c(x) = \phi_d\omega(x)d(x). \end{array}\right. \tag{1}$$

This article is protected by copyright. All rights reserved.

Accepted Article

where t [T] is the time and x [L] the distance to the channel varying from 0 at the river to L at the water divide. $S(x,t)$ [L^2] is the groundwater storage per unit length dx varying from 0 to the maximum groundwater storage $S_c(x)$ [L^2], $Q(x,t)$ [L^3/T] is the integrated Boussinesq groundwater flux, $N(t)$ [L/T] is the infiltration time series and $q_S(x,t)$ [L^2/T] is the saturation excess overland flow generated per unit length dx. $\mathscr{G}(u) = \mathscr{H}(u-1)$ and $\mathscr{R}(u) = u\,\mathscr{H}(u)$ are two functionals depending on the relative saturation (S/S_c) and flow balance ($-\dfrac{\partial Q}{\partial x}(x,t)+N(t)\,\omega(x)$) based on the Heaviside step function $\mathscr{H}$ to control the partition of incoming flux between water storage evolution and saturation excess overland flow (Figure 2.B, Marçais et al. (2017)).

The first equation of system 1 is the expression of the mass conservation for hillslope storage Boussinesq models (Troch et al., 2003). The second equation drives the local occurrence of saturation excess overland flow, when (1) groundwater storage saturates the whole aquifer column up to the surface $\mathscr{G}(\frac{S(x,t)}{S_c(x)}) = 1$ (2) positive incoming flux locally occurs, $-\dfrac{\partial Q}{\partial x}(x,t)+N(t)\,\omega(x) \geq 0$. At these conditions, the functional $\mathscr{R}$ is equivalent to the identity function (Figure 2.B) and $q_S(x,t) = -\dfrac{\partial Q}{\partial x}(x,t)+N(t)\,\omega(x)$. The third equation expresses the integrated groundwater flux $Q(x,t)$ over the transect made up of a Darcy flow driven by the gradient of storage and of a gravity flow function of the bedrock slope. Fourth equation relates the groundwater storage $S(x,t)$ to the hydraulic head $h(x,t)$. The last equation states that the groundwater storage S cannot be greater than S_c, since $h(x,t)$ is limited by the maximum aquifer depth $d(x)$. Runoff occurrence thus appears to be both bottom-up controlled by the saturation of the aquifer, through the development of variably saturated source areas and top-down controlled by the occurrence of infiltration events.

To take into account the routing process of the saturation excess overland flow and seepage flow, from the hillslope surface to the river, we developed a 1D gravity driven routing model (Text S1). In this study, as we focus on monthly discharge and transit time distribution dynamics, we consider that the discharge in the river can be approximated by $Q_{mod}(x,t) = Q(x,t)+\int_0^L q_S(x,t)dx$, assuming that, at the monthly timescale, saturation excess overland flow can be considered to be routed to the stream on much smaller time scales (Musy & Higy, 2004).

2.2 Transport model: stratifying groundwater flowpaths

2.2.1 A 2D stratified, advective transport

2D advective transport is modeled within a Lagrangian framework defining the flow lines over the whole domain. Horizontal groundwater particles velocity $v_x(x,t)$ directly derives from the Darcy flux Q integrated over the groundwater column (equation 3 of system 1), divided by the surface area of the porous section $\phi_{tot}\,\omega\,h$, where ϕ_{tot} is the total aquifer porosity. Replacing the aquifer depth h by the groundwater storage S using the penultimate equation of system 1, we get :

$$v_x(x,t) = \frac{\phi_d}{\phi_{tot}}\frac{Q(x,t)}{S(x,t)} \tag{2}$$

By applying mass conservation principles to the hillslope Boussinesq equations, we retrieve the vertical component of the particle velocities v_z and obtain the following La-

This article is protected by copyright. All rights reserved.

Accepted Article

grangian system of equations (see Appendix A):

$$\begin{cases} S(x(t),t)\dfrac{dx}{dt}(t) &= \dfrac{\phi_d}{\phi_{tot}}Q(x(t),t) \\ \dfrac{dz}{dt}(t) &= -z(t)\,\dfrac{\phi_d}{\phi_{tot}}\left(\dfrac{d}{dx}\left(\dfrac{Q(x(t),t)}{S(x(t),t)}\right)+\dfrac{1}{w}\dfrac{dw}{dx}\dfrac{Q(x(t),t)}{S(x(t),t)}\right) \\ x(t_0) &= x_0 \\ z(t_0) &= z_0 \;=\; h(x_0,t_0) \end{cases} \tag{3}$$

where t_0 is the initial time, $\mathbf{x_0} = (x_0, z_0)$ is the initial position of the flow line starting at the water table and $\mathbf{x}(t) = (x(t), z(t))$ is the 2D flow-line trajectory in the aquifer. With this novel description, the vertical component of the velocity field is derived from the horizontal velocity variations. Vertical transport of solutes is logically induced by variations of velocity in the other horizontal directions.

The transport equation (3) is solved by a particle method where $N_P = N_x N_t$ particles are injected for each of the N_t time steps at each of the N_x discretized elements. Each particle is seeded at the top of the saturated zone and is flux-weighted according to the intensity of the infiltration flux and to the relative area of the mesh cell (Figure S1). Particles are injected in the aquifer where aquifer saturation remains below the land surface, and at the surface otherwise.

For particles injected in the aquifer, this eventually leads to an aquifer stratification where transit times increase with depth. Older particles are deeper in the aquifer while the youngest ones, which have been just introduced through the most recent infiltration events, are above, closer to the water table (Figure 2). At each time t, particles crossing the groundwater boundaries (i.e. the water table and the imposed head boundary condition at the river) go from the groundwater compartment directly to the seepage areas or to the river. They correspond respectively to the seepage flow and to the baseflow (Figure 2). Their transit time is essentially equal to the time spent in the subsurface compartment $\tau_{gw}(t)$, as the transit time at the surface is much smaller. Particles injected at the surface are then assumed to have a transit time proportional to the distance to the stream from where they have been injected:

$$\tau_{surf}(x,t) = \frac{x}{L_{sat}} \min_{1\leq i\leq N(t)} \tau_{gw}^{i}(t) \tag{4}$$

where $\tau_{surf}(x,t)$ is the transit time of the particles injected directly at the surface, at a distance x from the river, $L_{sat}(t)$ is the length of the saturated extension, and $N(t)$ is the number of groundwater particles exiting at time t.

Due to the stratification obtained by the 2D trajectory description, seepage flow is fed first by the youngest particles, which are at the top of the groundwater column. Compared to other assumptions of full mixing over the water column, this method locates the streamline vertically, stratifies the transit times and correlates the depth of the streamline to the distance of its origin. Deeper streamlines originate from farther away. It has significant consequences on transit times. The youngest particles are the first to exit at the onset of the seepage area. The oldest particles are the last to leave and exit directly in the river. Overall the stratification increases the span of the transit time distribution. Equation (3) is solved in parallel with an implicit ode solver capable of managing the presence of a singularity in the case where $S(\mathbf{x}(t),t) = 0$. This is achieved

This article is protected by copyright. All rights reserved.

Accepted Article

with the variable time step and variable order ode15s MATLAB® solver (Shampine et al., 1999). The numerical methods are validated by comparing the flux-based modeled discharge Q_{mod} with the particular modeled discharge obtained by computing the particle flux reaching the stream at each time step (TextS2 and Figure S2). Results can be expressed as particle trajectories.

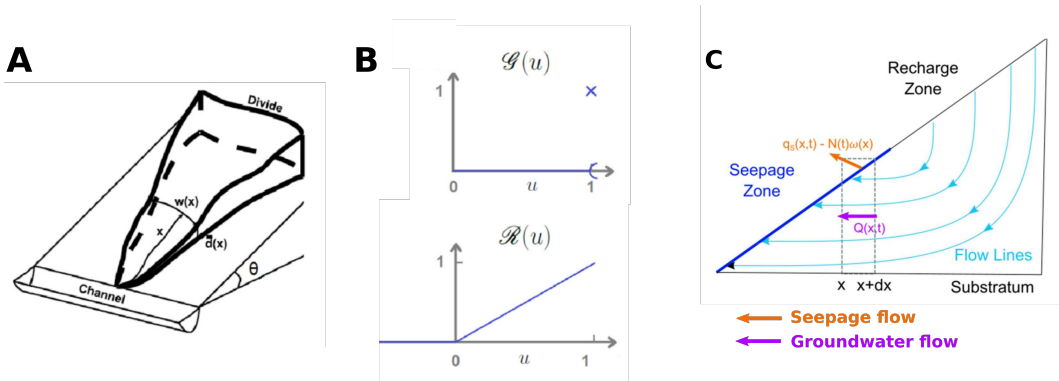

Figure 2. Sketch of A. the hillslope representation and geomorphologic variables ($\omega(x)$, the hillslope width, $d(x)$, the aquifer depth and $\theta(x)$, the hillslope bedrock slope), reproduced from Troch et al. (2003). B. the functions $\mathscr{G}$ and $\mathscr{R}$ used in the partitioning system of equations (1). C. the streamline organization. The stratification of the flow lines derived from the particle tracking method respects the conservation of mass laterally (in the direction modeled by the flux equation 1) and vertically through the premise of "no crossing" between streamlines. The strategy to retrieve seeping particles can be summarized as "last in, first out" for the particles, therefore suggesting a process-based interpretation for the preferential selection of young water discharged to the stream and to the seepage zone.

In the Boussinesq approach of groundwater flows, celerity (flux response to precipitation) is dissociated from velocity (effective particle speed inside the aquifer) due to three effects. First, the celerity response in time is only dictated by $Q(x,t)$ while the velocity response is driven by the ratio $\dfrac{Q(x,t)}{S(x,t)}$, meaning that the dynamics of stored drainable water also affect transport properties (Scaini et al., 2017). Second, the presence of a non-linearity due to the water table intersection with the land surface creates a responsive zone (the variable saturated areas) for flows, while the transport response is still predominantly controlled by the transit times of the particles travelling in the groundwater compartment. Third, it is the total amount of groundwater stored that effectively conditions the particle velocity by modifying the Darcy velocity with the ratio $\dfrac{\phi_d}{\phi_{tot}}$ (van Verseveld et al., 2017). In this model, these three effects contribute to dissociate celerity from velocity (McDonnell & Beven, 2014; McDonnell, 2017).

2.2.2 A longitudinal advective-dispersive transport scheme to model time variable residence time and transit time distributions

The numerical scheme introduced in the previous section corresponds to the 2D purely advective transport of a solute without any diffusion or dispersion. We introduce longitudinal diffusive and dispersive processes in the aquifer by considering that trans-

This article is protected by copyright. All rights reserved.

Accepted Article

port within each flow line can be modeled by an inverse Gaussian distribution accounting both for advective and diffusive/dispersive processes (Engdahl & Maxwell, 2014; Kirchner et al., 2001; de Marsily, 1986) (Text S3 and Figure S3). Dispersive and diffusive processes transversal to the flow lines are neglected because it is considered one order smaller than longitudinal dispersivity (de Marsily, 1986) and of second-order effects in such uniform media (de Dreuzy et al., 2007). For each particle with an age τ (which can be considered as a transit time or as a residence time depending on the medium sampled, stream or catchment), we obtain the following expressions for the distribution of transit times $p(t,\tau)$:

$$\begin{cases} p(t,\tau) &= \sqrt{\dfrac{25\tau}{4\pi t^3}}\exp\left(-\dfrac{25(t-\tau)^2}{4\tau t}\right) \quad \text{if} \quad t \geq 0 \\ p(t,\tau) &= 0 \quad \text{if} \quad t < 0 \end{cases} \tag{5}$$

The residence time distribution at time t can be derived from the residence time of all the particles k located in the aquifer and at the surface. The transit time distribution at time t is defined from the transit time of the particles i reaching the river between t and $t+\Delta t$. In both cases, the distribution of times is obtained by summing up the inverse Gaussian distributions centered on their individual traveling time τ^i in the aquifer and at the surface. Each of these inverse Gaussian distribution is weighted by the water volume associated to the particle. This results in synthetic, physically-based transient residence time distributions $p_S(t,\tau)$ and transit time distributions $p_Q(t,\tau)$.

2.3 Guillec catchment: field data and modeling strategy

To illustrate the value of this modeling approach, we assessed its relevance on the Guillec catchment located in western Brittany (France). The Guillec catchment has a relatively limited size (43 km^2). Discharge and CFC data are available. The Guillec catchment is characterized by an oceanic temperate climate with average precipitation of around 1000 mm/yr and real evapotranspiration approximately equal to 600 mm/yr. Its geology is crystalline, mainly granitic, though some siliclastic sedimentary materials are present in the fluvial system due to the weathering of the crystalline bedrock. Topographic gradients are relatively limited with altitudes ranging between 7 m and 125 m (Figure 3).

2.3.1 Flux data: monitored discharge and modeled infiltration data

Daily discharge time series are available over 54 years at the catchment outlet. With the objective to analyze the interannual and seasonal fluctuations of discharge and time-varying transit time distributions, the monthly average of this time series is derived. Input forcings for our modeling strategy come from the SURFEX land surface model (Le Moigne et al., 2020) seeded with SAFRAN atmospheric reanalysis (Vidal et al., 2010). SAFRAN provides precipitation and energy atmospheric forcings over France at the unified national scale (8x8 km^2 grid) (Quintana-Seguí et al., 2008). The SURFEX land surface model computes water and energy budgets in the soil compartment and produces precipitation, real evapotranspiration, runoff (shallow runoff) and drainage (deep infiltration) on the same national grid scale (Boone et al., 2017). To stick to our modeling framework, we summed runoff and drainage time series to provide a proper infiltration time series as the model itself spatially resolves the partitioning between infiltration excess overland flow and recharge (Marçais et al., 2017).

This article is protected by copyright. All rights reserved.

Accepted Article

Accepted Article

2.3.2 Transport data: sampling and interpretation of CFCs

Depending on the timescale of interest, an appropriate age tracer has to be chosen for groundwater dating (Suckow, 2014; Kazemi et al., 2006). Previous modeling studies in Brittany have estimated the mean streamwater transit times to be approximately 5 years to 7 years (Martin et al., 2006; Mougin et al., 2015). Groundwater mean residence times, which have been evaluated from CFC sampling in aquifers, show an older range, between 25 years (Marçais et al., 2018; Roques et al., 2014; Ayraud et al., 2008) and 50 years (Kolbe et al., 2016). Groundwater inputs to streams are significant, from 30 % to 60 % of the stream discharge (Clément et al., 2003; Mougin et al., 2002, 2008; Aquilina et al., 2012). A first-order analysis shows apparent inconsistencies between these observations at least when they are compared to regional scale estimates, as a 50 % input of 25 year old groundwater to streams would lead to streamwater mean transit times of at least 12.5 years. As we are interested in understanding the contribution and age of groundwater to the Guillec river, we chose CFCs to date groundwater because CFC ages are sensitive to time scales of years to decades.

CFCs are assumed to be in equilibrium with the atmosphere in the unsaturated zone, provided that the water table is not too deep (typically not more than 5m)(Engesgaard et al., 2004), which is generally the case for Brittany (Mougin et al., 2004; Kolbe et al., 2016). Once the infiltrating water recharges the aquifer, it becomes isolated from the atmosphere, with the dissolved concentration equilibrated with the atmospheric concentration at the time of isolation. CFCs are then assumed to be transported conservatively in the aquifer. For this analysis, we sampled the two wells shown as violet circles on Figure 3A and the Guillec river close to its outlet (blue triangle). We calibrated the transport model on these three CFCs samples. Aerobic conditions prevent CFC degradation (Dunkle et al., 1993; Kolbe et al., 2020). In any case, exchanges between the samples and the atmosphere have been minimized, by sampling far from the river re-aeration zones and at the very bottom of the water column (Vautier et al., 2020; Guillaumot et al., 2021). The two wells were chosen because they are known to be located just upstream of well-identified springs. Sampled waters are thus confirmed to characterize the contribution of the aquifer to the stream. In the river, we sampled CFCs at the end of the low flow period in October to ensure both significant river depth and a majority of streamwater coming from the aquifer.

CFCs were analyzed at the CONDATE Eau facility of the University of Rennes, France (OSUR laboratory) (Ayraud et al., 2008; Labasque et al., 2014). CFC-11 and CFC-113 concentrations were found to be consistent with each other and were retained as modeling targets, except one contaminated CFC-11 sample (Table S1). In contrast, most CFC-12 concentrations appeared to be contaminated as the values were well above the maximum atmospheric concentration ever recorded.

2.3.3 Topographic data: an equivalent hillslope representation

The hillslope model has been derived on the basis of the topographically defined catchment from the gauging station at the outlet (Figure 3A). SRTM data (Farr et al., 2007) were analyzed with the topotoolbox package (Schwanghart & Scherler, 2014) under the assumption that the hydrological and hydrogeological catchments correspond (Reggiani et al., 1998; Reggiani & Schellekens, 2003; Haitjema & Mitchell-Bruker, 2005; Gleeson & Manning, 2008). This assumption is generally appropriate in Brittany where limited

This article is protected by copyright. All rights reserved.

weathering of the crystalline bedrocks and low topographical gradients preclude the existence of significant regional groundwater circulation (Kolbe et al., 2016). We chose to rely on a representation of the catchment based on an equivalent hillslope representation characterized by its relative elevation to the river (Loritz et al., 2017; Reggiani & Schellekens, 2003). This equivalent hillslope is obtained by aggregating the cells of the DEM in a 1D representation according to their distance to the river in the DEM (Figure 3B and C). The slope of its surface is relatively limited to be around 2.5 %. The 2D DEM-based analysis gives the width function and the mean elevation function at the scale of the catchment. Assuming a flat bedrock located at the same elevation as the river outlet (L'vovich, 1979), the width and elevation functions characterize the storage capacity of the catchment S_{tot} (which we assumed to be mainly located in its shallow aquifer) as a function of the distance to the stream: $S_{tot}(x,t) = \phi_{tot}\,\omega(x)\,d(x)$.

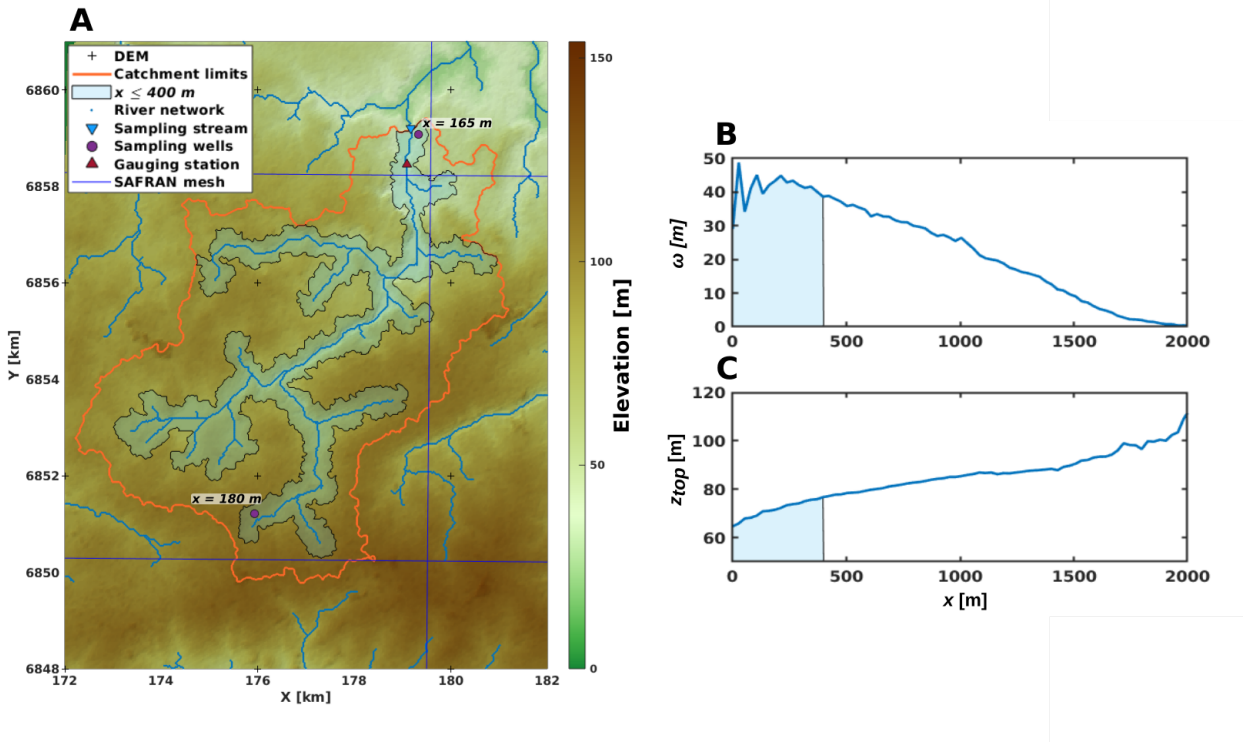

Figure 3. (A) 2D representation of the topography of the Guillec catchment with the sampling locations indicated as circles and triangles. The distance of the sampled locations to the river are indicated in black. The gridding mesh used to retrieve infiltration time series from the SURFEX model is superimposed in blue. (B) Width function $\omega(x)$ and (C) elevation function $z_{top}(x)$ of the equivalent hillslope characterizing the repartition of the catchment area as a function of the distance x to the stream. To illustrate the aggregation strategy, we highlight the elevation and the width of the equivalent hillslope in pale blue for a distance to the stream smaller than 400 m. Corresponding DEM cells are highlighted with the same color in (A).

This article is protected by copyright. All rights reserved.

Accepted Article

2.3.4 Model calibration

The model has 3 parameters to calibrate, which are the bedrock hydraulic conductivity k, the bedrock drainable porosity ϕ_d and the bedrock total porosity ϕ_{tot}. According to the available data, our strategy is first to select the most promising flow models defined by their hydraulic conductivity k and their drainable porosity ϕ_d with the monthly discharge observations and second to determine the total aquifer porosity ϕ_{tot} with the sampled CFCs measurements.

Flows are modeled by the methods given in section 2.1 with a finely discretized mesh of 500 cells (4m wide). We calibrated the flow model parameters, i. e. the aquifer hydraulic conductivity k and the drainable porosity ϕ_d, on the monthly discharge time series. We ran 25,000 simulations with a Monte Carlo sampling method, k in the range $[10^{-8}, 10^{-4}]$ m/s and ϕ_d in the range $[0.005, 0.5]$. The goodness of fit is assessed by the Kling-Gupta efficiency (KGE) (Gupta et al., 2009). KGE increases for better models and reaches 1 for a perfect fit.

We selected the 39 best simulations giving the highest KGE values and ran the advective-dispersive transport on them for different ϕ_{tot} values in $[\phi_d, 0.5]$. This resulted in 147 transport simulations on which CFC-11 and CFC-113 concentrations ($C^{mod}_{CFC}(t_s, x)$ expressed in equivalent to atmospheric concentration, where t_s is the sampling time and x is the distance of the sampling location to the river) are estimated in the river and in the wells, under the assumption of no atmospheric contamination, with the classic convolution equation (Marçais et al., 2015). We then calibrated the hillslope transport model on the CFC concentrations, by minimizing the following objective function:

$$\Theta(k, \phi_d, \phi_{tot}) = 1 - \frac{1}{6}\left(\frac{\sum_{i=1}^{3} |C^{mod}_{CFC11_i}(x_i) - C^{obs}_{CFC11_i}(x_i)|}{\sum_{i=1}^{3} |C^{obs}_{CFC11_i}(x_i)|} + \frac{\sum_{i=1}^{3} |C^{mod}_{CFC113_i}(x_i) - C^{obs}_{CFC113_i}(x_i)|}{\sum_{i=1}^{3} |C^{obs}_{CFC113_i}(x_i)|} \right) \tag{6}$$

Like the KGE indicator, Θ gets close to 1 for perfect fits.

3 Results

We present the calibration results and the capacity of the discharge and CFCs data to constrain the aquifer hydraulic parameters (section 3.1). The calibrated models show the control of the streamwater mean transit times by the groundwater contribution (section 3.2) and illustrate its seasonal evolution with the dynamic partitioning of the overland flow, seepage flow and baseflow (section 3.3).

3.1 Calibration of the aquifer hydraulic parameters

3.1.1 Calibration of the hydraulic conductivity by discharge data

Hydraulic conductivity k and drainable porosity ϕ_d are evaluated by comparing the observed and simulated discharge data at the Guillec catchment outlet according to the KGE metric (Figures 4.A, S4, S5 and Text S4). The modeled discharge is highly sensitive to both k and ϕ_d with KGE values broadly ranging between 0.040 and 0.82. The local maximum values of KGE are underlined by the dashed red curve and cover a wide

This article is protected by copyright. All rights reserved.

Accepted Article

range of k and ϕ_d values organized around two trends respectively horizontal and vertical (Figures 4.A, S6 and Text S5). For the vertical trend, k is well constrained around 10^{-5} m/s while ϕ_d broadly varies between 2 % and 47 %. For the horizontal trend, ϕ_d is smaller around 1 % while k varies between 10^{-5} m/s and $9{\times}10^{-5}$ m/s. It shows that discharge data constrain the hydraulic conductivities within less than one order of magnitude (from $1{\times}10^{-5}$ m/s to 9×10^{-5} m/s) out of the 4 orders of magnitude explored (from 10^{-8} m/s to 10^{-4} m/s). The drainable porosity ϕ_d is however poorly constrained with the best simulations spanning almost all the explored range, from 0.6 % to 47 %. At this stage, We select the 39 sets of parameters (k,ϕ_d) giving the best KGE values (i.e. $KGE \geq 0.8$, indicated by dots on Figure 4.A).

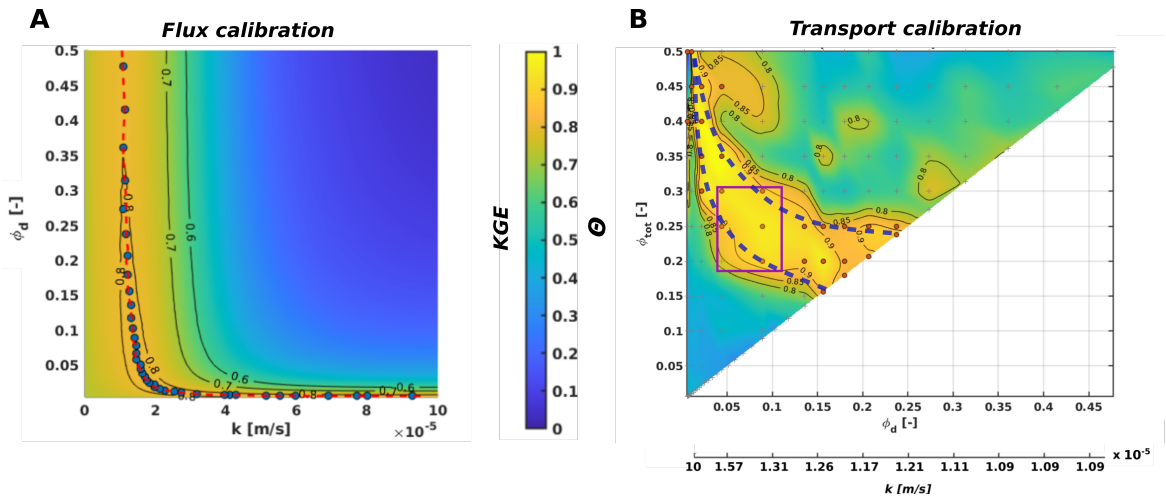

Figure 4. A. KGE calibration performance on discharge data displayed for the 25 000 simulations sampling the (k,ϕ_d) parameter space. The dotted red curve indicates the location of the local maxima joining the 39 best models retained for the analysis (blue dots). B. Θ calibration performance on CFCs data (6) in the (ϕ_d,ϕ_{tot}) space. Orange circles represent the 28 best transport models. Dashed blue lines materialize the constrained zone in the (ϕ_d,ϕ_{tot}) map. The purple rectangle further restrains the acceptable values within the range of values previously reported in the literature for the same type of lithologies (section 4.1). In the right figure, values of the hydraulic conductivity k corresponding to the drainable porosity ϕ_d (obtained from the calibration of the discharge data, section 3.1) are represented on the lower scale (scale is not linear).

3.1.2 Calibration of drainable and total porosities by CFCs data

Starting from the 39 best flow models obtained with the previously identified (k, ϕ_d) sets, we defined 147 transport models with different values of ϕ_{tot} to explore the parameter space defined by $\phi_{tot} \geq \phi_d$. We assessed the agreement between modeled and sampled CFC concentrations with the function Θ (equation 6 and Figure S7). Results show that a close match is obtained for 28 of the 147 models with values of Θ greater than 0.8 defining a characteristic zone of acceptance in the (ϕ_d,ϕ_{tot}) space (Figure 4.B). By construction, the 28 models match both the sampled CFC concentrations and the seasonal discharge variations.

This article is protected by copyright. All rights reserved.

Accepted Article

ϕ_d and ϕ_{tot} are partly constrained by CFC data (dashed blue lines on Figure 4.B), while they were not by the discharge data. Admissible ϕ_d and ϕ_{tot} lead to streamwater mean transit times equal to 13±2 years (Figures 5.B, S8 and S9). Any decrease of the drainable porosity ϕ_d is balanced by some increase of the total porosity ϕ_{tot} to compensate the speed up of the drainable flowpaths by some additional delay in the immobile porosity ($\phi_{tot}-\phi_d$). ϕ_d and ϕ_{tot} do not however have exactly the same effect. ϕ_d modifies the speed of the drainable flowpaths, the dynamical storage of the aquifer and its seasonal amplitude as well as the water table intersection with the topography and its dynamic. In contrast, ϕ_{tot} more directly scales the transit times (equation 3) through a simple linear dependency, which clearly appears at steady state (Text S6 and Figure S8).

3.2 Controls of streamwater mean transit times by groundwater contributions

The contribution of groundwater to the streams is characterized by the Groundwater Index. The Groundwater Index, abbreviated GWI, is defined as the proportion of baseflow and seepage flow to the streamflow. It is on average equal to 75 % with a limited variability among the 39 best models (± 14 %, Figure 5.A). When it reaches the stream, groundwater is on average 17±3.5 years old (Figure 5.B). As a result, streamwaters are relatively old with a mean transit time of 13 years ($\approx 17 \times 0.75$) assuming that overland flows are less than 1 year old and intervene mostly through a dilution effect. Even in the wet season when its contribution is reduced, groundwater still amounts to 40 % of the stream discharge, explaining why streamwater transit times remain "old" ($\approx$ 6.6 years old).

Resulting from the Boussinesq response and from the seasonal water table intersection with the topography, GWI, the groundwater contributions to the stream varies significantly throughout the year. GWI decreases from 0.98 at early low flows (August), when streams are almost exclusively fed by aquifers, to 0.39 at early high flows (December), when precipitation and saturated areas are maximal (Figure 5.A). The streamwater mean transit time (mTT) displays similar variations with a time lag of 1-2 months, from 20 years at late low flows (October) to 6.5 years at the late high flow season (February) (Figure 5.B). The mean transit time of the groundwater contribution to the stream (mTT_{gw}) is further delayed by one month ($mTT_{gw} \in [14.5, 33]$ years). This is because deeper compartments of the catchment have a delayed response compared to the shallower compartments. mTT_{gw} also displays an increased variability between the calibrated models (± 3.5 years for mTT_{gw} to compare with ± 1.7 years for the mTT).

This shows that the groundwater contribution characterized by GWI, which is controlled by the aquifer hydraulic conductivity k (section 3.1.1), itself controls the seasonal dynamics of streamwater mean transit times mTT. Below, we further investigate the effect of flowpath decomposition on the full transit time distribution (TTD) and its seasonal variations.

3.3 Structure of the Transit Time Distributions as revealed by the flowpath organization

The decomposition of the transit time distribution in these three flowpath components (overland flow, seepage flow and baseflow) shows how the spatial stratification of

This article is protected by copyright. All rights reserved.

Accepted Article

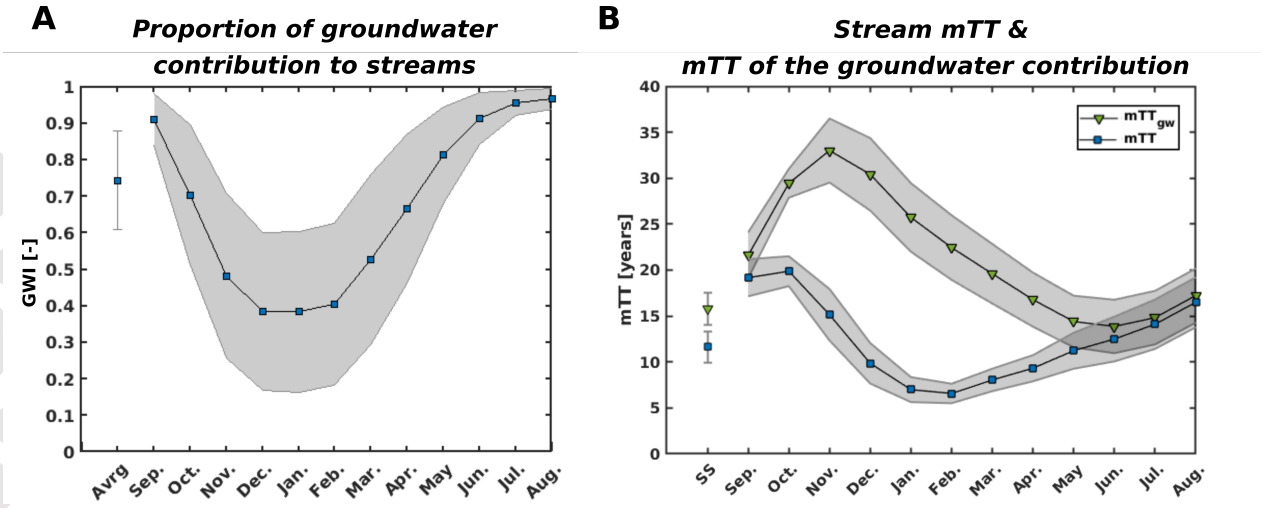

Figure 5. Modeled interannual monthly variations of A. the proportion of groundwater contributions to stream characterized by the Groundwater Index GWI and B. the streamwater mean transit times (mTT, squares) and mean transit times of the groundwater contribution to stream (mTT_{gw}, triangles). Note how the contribution of the aquifer is delayed compared to the river signal. The maximum mTT_{gw} is reached in November, one month later than mTT (maximum attained in October). The shaded area marks the standard deviation obtained with the 28 best transport models (out of 147 transport models). First points and error bars on the left labeled "Avrg" and "SS" stand respectively for the annual average and for the steady state value.

the flowpaths is translated in the time domain both in low flow and high flow periods (Figure 6.A). Overland flows have the fastest times centered on one month (0.1 year) (red curves). Seepage flows have an intermediate timescale centered on one year (green curves). This timescale of one year reflects the seasonal seepage front development at the top of the aquifer composed of groundwater with a residence time less than one year since it is flushed every year. Third, the baseflow contribution has the oldest transit times with an average timescale of 10 to 30 years depending on the season (blue curves).

Differences in the TTD decomposition between seasons (at high flow vs low flow) lead to some counterintuitive results. At high flows (curves indicated by diamonds), the transit times of the overland and seepage flows are surprisingly slightly longer than at low flows. It results from the development of the seepage zone and reflects the fact that runoff occurs from farther away from the river on the hillslope increasing the mean transit time of overland flowpaths to the river. With receding seepage (crosses), flowpaths emerging in the seepage zone become shorter by occurring closer to the stream. Similar conclusions have been drawn by Wilusz et al. (2020). More intuitively, baseflow contribution is older at low flows as it comes from deeper older compartments due to the groundwater age stratification. Interestingly, the transit time distributions of the baseflow contribution is the most sensitive to seasonal variations with transit timescales significantly shifted from high flow (10 years) to low flow (30 years), in line with the mTT_{gw} seasonal variations (triangles in Figure 5.B).

However, we observe that the large seasonal mean transit time variations (squares in Figure 5.B) do not result from the intrinsic mTT variability of the different flowpath

This article is protected by copyright. All rights reserved.

Accepted Article

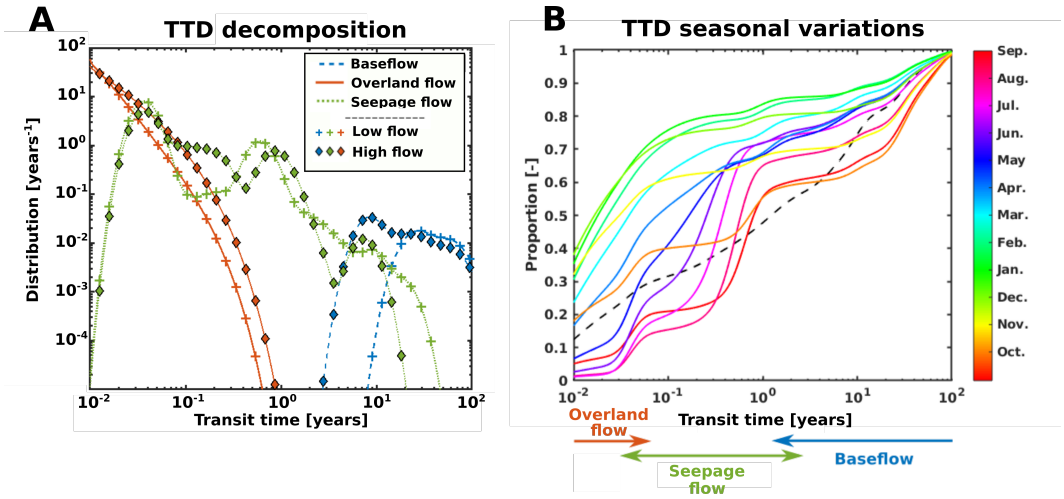

Figure 6. A. TTD decomposition in the streamflow components illustrated by Figure 1: overland flow (red solid lines), seepage flow (green dotted lines) and baseflow (blue dashed lines). TTDs are given at low flows in September 2016 (crosses) and at high flows in February 2017 (diamonds). B. Interannual averaged seasonal cumulative TTDs. During the wet season, the proportion of young water in the river increases significantly. The black dotted line represents the steady state transit time distribution. Transport simulation were obtained for $k = 1.6 \times 10^{-5}$ m/s, $\phi_d = 4$ % and $\phi_{tot} = 25$ %. Note the well-separated characteristics transit times of the three flow components on both figures.

components (overland flow, seepage flow or deep flow), but rather from the time-varying respective contribution of these fluxes to the stream discharge, in accordance with previous studies carried with the SAS framework (Rodriguez & Klaus, 2019; Wilusz et al., 2020). The seasonal variations of the cumulative transit time distributions shown by Figure 6.B confirm this. On this plot, the lines of the cumulative TTDs indeed display sharp increases at specific transit timescales illustrating shifts in the relative proportion of these flowpaths.

4 Discussion

4.1 Complementarity of discharge and CFCs data informs catchment scale hydrological properties and processes

Discharge data turn out to illuminate hydraulic conductivity at the catchment scale by constraining its range to less than one order of magnitude between 10^{-5} m/s and 9×10^{-5} m/s. Such values of hydraulic conductivities are consistent with previous ranges of hydraulic conductivities and transmissivities obtained at comparable scales for the crystalline basements of Brittany as shown by Table 1 (Conan et al., 2003; Grimaldi et al., 2009; Molenat, 1999; Clément et al., 2003; Legchenko et al., 2004; Martin et al., 2006; Kolbe et al., 2016; Leray et al., 2012; Le Borgne et al., 2006; Roques et al., 2014). The limited range of estimated hydraulic conductivity and the agreement with independently derived values show that this method adequately constrains hydraulic conductivities at the catchment scale. It offers a complementary approach to the classic analysis of recession first introduced by Brutsaert and Nieber (1977), which requires essential but difficult-

This article is protected by copyright. All rights reserved.

Accepted Article

to-assess assumptions for extracting the baseflow contribution (Wittenberg & Sivapalan, 1999; Troch et al., 2013; Vannier et al., 2014).

Fundamentally, the limited range inferred for the hydraulic conductivity comes from the sensitivity of the partitioning process between overland flows and groundwater flows in the discharge data. The contribution of baseflow and seepage flows sustaining the river discharge, estimated on average at 75 %, is indeed consistent with previous first-order estimates of around 60 % (Mougin et al., 2008; Aquilina et al., 2012; Clément et al., 2003) as well as with statistical filter estimates of around 79 % (Gustard et al., 1992; Lyne & Hollick, 1979). The contribution of overland flows is directly controlled by the distribution of saturation along the hillslope (Kosugi et al., 2008; Montgomery et al., 1997; Wilson & Dietrich, 1987; S. P. Anderson et al., 1997), which is set by the water table position relative to the surface. At first order, this position of the water table is controlled by the hydraulic conductivity and not by the drainable porosity. This is intuitively illustrated by the absence of dependence of the steady-state groundwater flow equation on the drainable porosity. The drainable porosity only intervenes as a second-order control for the typical seasonal dynamics of the water table and the subsequent seasonal baseflow contributions to the streamflow (Figure S8). This effectively explains why the drainable porosity range cannot be constrained by the discharge datasets alone (Guérin et al., 2019). It also explains why the overall model uncertainty is not strongly impacted by the uncertainty of the drainable porosity.

k [m/s]	T [m^2/s]	ϕ_d [-]	ϕ_{tot} [-]	Depth [m]	N	Settings	Reference
1.8 10^{-5}	**3.1 10^{-4}**	**0.080**	**0.29**	**17**	**28**	**Guillec: shallow granites**	**This study**
8.0 10^{-6}		0.080	0.60	20	12	Kerrien, Kerbernez: shallow granites	Martin et al. (2006)
3.6 10^{-5}		0.050		30	10	Kerrien, Kerbernez: shallow granites	Legchenko et al. (2004)
1.0 10^{-5}				10	2	Pleine Fougeres: weathered schists	Clément et al. (2003)
6.3 10^{-6}			0.45	20	10	Pleine Fougeres: weathered schists and granites	Kolbe et al. (2016)
2.6 10^{-6}			0.21	50	10	Pleine Fougeres: fractured schists and granites	Kolbe et al. (2016)
5.1 10^{-6}		0.030		6	7	Kervidy: weathered schists	Molenat (1999)
2.2 10^{-6}					4	Pont Lagot: weathered schists	Grimaldi et al. (2009)
1.0 10^{-5}		0.013			2	Kervidy: weathered schists	Conan et al. (2003)
	1.3 10^{-5}				2	Kervidy: fractured schists	Conan et al. (2003)
	2.2 10^{-3}	0.037			11	Plœmeur: transmissive zone, schists and granites	Leray et al. (2012)
	6.0 10^{-4}			≤ 25	12	Plœmeur: shallow schists	Le Borgne et al. (2006)
	2.2 10^{-4}			≥ 25	22	Plœmeur: deep granites	Le Borgne et al. (2006)
	2.9 10^{-3}				23	Plœmeur: schists and granites	Le Borgne et al. (2006)
	7.3 10^{-5}	0.035		15	4	St Brice: weathered schists	Roques et al. (2014)
	4.4 10^{-4}			50	7	St Brice: fractured schists	Roques et al. (2014)

Table 1. Logarithmic averaged measured or modeled hydraulic properties in Brittany aquifers. For each site, independent estimates are provided as well as typical depth of investigation when available. N is the number of independent values leading to these estimations. For more details, see Text S7.

Drainable and total porosities can however be at least partially constrained by CFC data. The drainable porosity ϕ_d must be between 0.6 % and 25 %, and the total porosity ϕ_{tot} between 15 % and 47 % (Figure 4.B). Such ranges are consistent with previous studies from which the drainable porosity inferred from well pumping tests or geochemical characteristics has been found between 2 % and 10 % (Legchenko et al., 2004; Martin et al., 2006; Molenat, 1999; Leray et al., 2012; Roques et al., 2014) and the total porosity inferred with CFC data between 25 % and 45 % (Kolbe et al., 2016) (see Table 1). With these values, the porosities of the Guillec catchment would be further constrained

This article is protected by copyright. All rights reserved.

Accepted Article

between 3 % and 12 % for ϕ_d and between 20 and 30 % for ϕ_{tot} (see purple rectangle on Figure 4.B). The range of ϕ_{tot} might be quite high if not considering that the total porosity is a lumped way to represent the different processes and structures that delay the transport of solutes (Haggerty & Gorelick, 1995; Carrera et al., 1998).

4.2 The seasonal water table intersection with the land surface drives the dynamics of the mean transit time mTT

The streamwater mean transit time mTT is equal to 13 years, almost twice as large as the 7 years estimated previously on similar sites based on renewal rates (Mougin et al., 2015). Even though it is controlled by the averaged size of the groundwater storage like in other similar sites (Kolbe et al., 2016; Haitjema, 1995; Chesnaux et al., 2005), the mean transit time differs from the renewal rate defined as the groundwater storage divided by the recharge (Danckwerts, 1953). Two of the assumptions underlying the renewal rate approximation noted in Harman (2014) and Berghuijs and Kirchner (2017) are not fulfilled. First, the modeled processes are inherently transient. Differences between the steady state (i.e. obtained when the state variable S does not vary) and the stationary state (i.e. the average of the seasonal variations) mTT and mTT_{gw} are significant (Table S2). This is also clearly illustrated on Figure 7, where the steady state mean transit time of the groundwater contributions to the stream mTT_{gw} is significantly shorter than the seasonal mTT_{gw} variations. This comes from the non linearity of the model incorporating seepage areas that strongly depend on the precise water table location. Detailed explanations are given in Text S8. Second, the reservoir is not perfectly mixed. The transit time distribution is therefore rather power-law than exponential because the reservoir remains stratified with only partial mixing and is limited at the water table by the seasonal intersection with the land surface.

These results confirm the measurements carried out regionally on several Brittany watersheds and more globally in temperate catchments (J. Yang et al., 2018). From a depth of a few meters below the water table, the residence time is greater than 10 years, but conversely, the yearly-flushed, variably saturated zone shows residence times on the order of one year (Ayraud et al., 2008; Legout et al., 2007; de Montety et al., 2018). The results obtained here make it possible to remove a contradiction between the observations of residence times measured by tracers in groundwater which indicate long times and the fast processes generally associated with streamwater discharge dynamics. Long residence times in groundwater (through baseflow) together with a rapid component of transfer into the rivers (trough overland and seepage flow) are not incompatible, rather they are linked through the seasonal water table fluctuations and groundwater stratification.

We further explore how these modeled processes control the temporal dynamics of the mean transit time mTT. To highlight their impact on the model results we perform two complementary simulations where we alternatively remove water table intersection and stratification from the reference model (squares in Figure 7). The reference model refers to the model, which has been used in this study (described in section 2). First, we removed the water table interactions with the land surface (stars in Figure 7) from the reference model by not considering the upper land surface boundary on the aquifer capacity (last equation of system of equations (1)). For this model, the seasonal dynamics of mTT almost vanishes with variations strongly limited to 1.7 years (Figure 7.A).

This article is protected by copyright. All rights reserved.

Accepted Article

Second, we removed the groundwater stratification (diamonds in Figure 7) from the reference model. To do that, we relaxed the implicit condition stated in the second equation of system (3) that the particles exiting the first the aquifer at the seepage face are the ones located at the top of the aquifer column. Instead, we developed an algorithm that randomly samples particles, from any vertical location of a given numeric cell encountering seepage face. The right number of particles is retrieved to feed the seepage flux by ensuring flux conservation. For this latter model, the seasonal dynamics of the mean transit time is well preserved as well as its magnitude. The remaining differences mainly occur during the dry season (±4 years at most during the September month) when transit times are dominantly controlled by the proportion of groundwater contributions to streamflow.

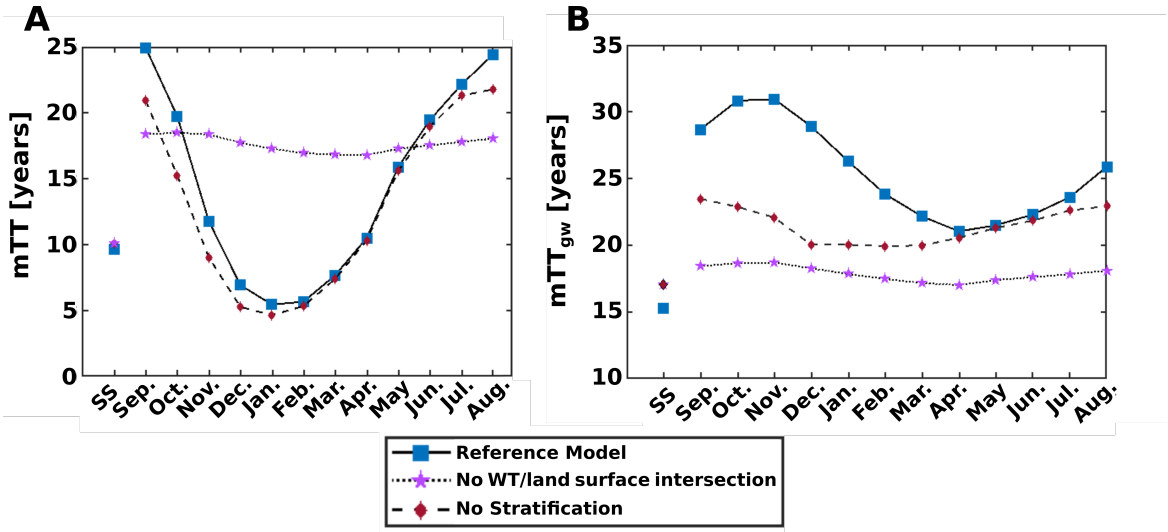

Figure 7. Investigation of the relative effects of the seasonal water table intersection with the land surface and of the groundwater flowpaths stratification for the steady state (SS) and interannual monthly averaged. Comparison of A. the mean transit time to the river mTT and B. the mean transit time of the groundwater contribution (baseflow and seepage flow) to the streamwater mTT_{gw} for the reference model (squares) and the models without intersection with the surface (stars) and without groundwater stratification (diamonds). The three models are parametrized with: $k = 1.17\,10^{-5}$ m/s and $\phi_d = \phi_{tot} = 24$ %. Note that the difference of vertical scales between the two figures.

Two compartments (here the surface and the aquifer), with different characteristic transit times, are therefore needed to obtain seasonally varying mTT. Their dynamical connection through water table intersection indeed generates temporary saturation excess overland flow and seepage flow leading to seasonally varying mTT. With only the groundwater compartment, the seasonally varying infiltration fluxes are dampened by the groundwater storage volume and mTT becomes nearly constant. Groundwater stratification alone has a notably smaller impact on the streamflow mTT since mTT variations are primarily controlled by the relative contribution of groundwater flows to the stream and not by the internal organization of groundwater circulation inside the aquifer.

This article is protected by copyright. All rights reserved.

Accepted Article

Here the short streamwater transit times come from the contribution of the surface compartment to the stream. While the groundwater compartment is key to explain the old transit times ($\geq$ 1 year old), faster flowpaths can be delivered by the surface or by the soil compartment. Deciphering the relative role of these shallower compartments would require other tracers than CFCs and a model running with finer timesteps (e.g. hourly to daily timesteps).

4.3 Groundwater flowpath stratification is critical for the mean transit time of the groundwater contribution to the river mTT_{gw}

While groundwater stratification is a second-order control of the mean transit time dynamics of the entire streamflow, it becomes essential for the mean transit time dynamics of the groundwater contribution to the river, mTT_{gw} (Figure 7.B). The simplified model without stratification (diamonds) misses the seasonal dynamics of the reference hillslope model (squares). Indeed, for the reference model, mTT_{gw} broadly varies by ± 4 years around a mean of 27 years. On the contrary, the model without groundwater stratification only varies by ± 1.5 years around a mean of 23 years. Randomly sampling the particles from the water column indeed removes the preference for the aquifer to release young water. On the contrary, the reference model, which respects the stratification of groundwater residence times, mostly samples young groundwater during the wet season, when such young particles are available at the top of the water column. During the dry season, only old groundwater particles remain to be sampled, reinforcing the seasonal variability of mTT_{gw}.

The quantity mTT_{gw} is likely to be crucial when a precise representation of deep compartments is needed. This encompasses a broad range of topics, from studies assessing the impact of global climate change on transit times and water quality to studies interested in legacy effects of these groundwater storages, including geochemical processes where the interaction of reaction kinetics and transit times can be important (White et al., 1983). Both measured and model-derived water ages have been shown to correlate with weathering-derived solute chemistry in streams (Benettin et al., 2015; Rademacher et al., 2005). Geochemical tracer data such as Ge/Si ratios and stable isotopes of Si and Ca indicate that not only the flux but also the sources of solutes vary with discharge in studied streams (Kurtz et al., 2011; Cenki-Tok et al., 2009). The mechanism can include interactions with different materials along different flowpaths, but also differences in the time available for reaction progress as in kinetically limited systems (Fernandez et al., 2021). Integrated hydro-biogeochemical models, like the approach outlined here, relying on partitioning flow and timing transport are therefore needed to address these hypotheses.

4.4 Limitations and perspectives

While this parsimonious strategy effectively constrains the transit times of the groundwater circulation, some limitations arise from the conceptual representation of the surface and unsaturated zone processes. First, surface runoff processes are represented through a gravity-driven routing representation. This routing scheme neglects pre-event water present in the soil matrix , which can contribute to the flow. The presence of pre-event water could delay the estimated transit times of overland flowpaths by some months but will not significantly change the estimate of the mean transit times and the old compo-

This article is protected by copyright. All rights reserved.

Accepted Article

nent of the streamwater transit times distributions. However, this limitation prevents us from applying the model in its current configuration at the daily to hourly timescale. Indeed, we would strongly underestimate runoff routing transit times that have been shown to be mainly made up of pre-event water (von Freyberg et al., 2018). Adding a more detailed runoff component but still parsimonious to this equivalent hillslope representation could be achieved through a total soil water storage description that could be partially mixed with the runoff routing. This would also enable the model to distinguish between the fast flowpaths arising at the surface or in the soil compartment (Heidbüchel et al., 2020). Second, this routing scheme process neglects re-infiltration typically occurring before surface overland flow reaches the stream (Jackson et al., 2014; Klaus & Jackson, 2018; Gabrielli & McDonnell, 2020). In our model, most of the saturation excess overland flow is generated in the vicinity of the river. This proximity to the river might prevent re-infiltration (Jackson et al., 2014). Nevertheless, if re-infiltration occurs here, increased transit times would be less than one year as the groundwater transit times for water infiltrating in the vicinity of the river is less than one year (Figure S10).

Another limitation refers to the transfers in the unsaturated zone, which have been neglected. Studies of transit times in the unsaturated zone in crystalline basement have shown that they are short (ca. 2 years) (Legout et al., 2007; de Montety et al., 2018), and so integration of an explicit representation of unsaturated zone transfer should have marginal impact on the longer transit times associated with groundwater flow. Indeed, in crystalline basements located in temperate climate, the unsaturated zone is quite shallow (typically less than 5 meters, (Le Borgne et al., 2006; Roques et al., 2014; Marçais et al., 2018)). This could be different for other settings (arid climate, sedimentary settings), where the representation of percolation in the unsaturated zone will be a significant part of the total transit times to the stream (Schwientek et al., 2009; Green et al., 2018; Chen et al., 2019). Adding a flux and transport representation of the vadose zone could be done with a 1D vertical model, which would preserve the parsimonious philosophy of the approach presented here for the saturated compartment (Harman et al., 2011).

All these limitations would increase the young transit times, but would have only small effects on the old transit times. Further, constraining these fast processes would require the addition of specific tracers well-suited for short transit times. Indeed, CFCs tracers cannot track transport in the unsaturated zone and are not adapted to the timescales below one year, which require intensive monitoring of stable water isotopes (^2H, $\delta^{18}O$) or conservative solutes (chloride) (Sprenger et al., 2019; Harman, 2014; Benettin, Soulsby, et al., 2017).

An additional limitation in this study is related to the number of CFCs samples used to calibrate the model. We only relied on one sampling campaign on three different sampling sites to date the groundwater and its contribution to the river. A solution would be to sample more sites, e.g. by systematically sampling springs (Rademacher et al., 2001, 2005) or to sample CFCs at different seasons (Guillaumot et al., 2021). More intensive sampling indeed enables to link discharge (Morgenstern et al., 2010) or dissolved solutes concentrations to groundwater ages (Marçais et al., 2018), which offers opportunities to strengthen the spatial and temporal resolution of transit times in the river (Peters et al., 2014).

This article is protected by copyright. All rights reserved.

Accepted Article

Accepted Article

5 Conclusion

Using a parsimonious approach that emphasizes 1) variable contributions from shallow and deep flow paths and 2) stratification of groundwater residence times, we have demonstrated how the groundwater contribution to streams control streamwater mean transit times and its seasonal variations in a crystalline bedrock catchment under temperate climate. The 2D model requires the calibration of the hydraulic conductivity, drainable porosity and total porosity from discharge time series and CFC data. In the catchment studied, all the calibrated models display significant groundwater contribution to stream (ca. 75±14 %) with an average age of 17 years, leading to mean streamwater transit times on average equal to 13 years. All calibrated models display strong seasonal interactions between the water table and the land surface leading to a dynamic partitioning between groundwater flows (baseflow + seepage flow) and overland flows. This partitioning strongly conditions the seasonal dynamics of the streamwater mean transit times, from 6 years at high flow to 20 years at low flow.

The influence of the groundwater residence time stratification plays only a second-order role for the seasonal evolution of streamwater mean transit times, but is significant for the seasonal evolution of the mean transit times of the groundwater contribution to the stream. This last finding is likely to play a pivotal role for compounds which are predominantly found or generated in the aquifer. These may include solutes released from bedrock weathering or contaminants transported in groundwater.

The hillslope models show how (1) surface vs groundwater flow partitioning and (2) groundwater residence time stratification shape the transit time distributions. The understanding obtained through this study is particularly important for issues related to diffuse pollutant transfers and more generally to element transfers and biogeochemical fluxes within catchments. It is common for workers in the field to focus on in-stream processes and rapid dynamics that impact river flow, such as overland flow. Here we show that most of the streamwater has in fact resided underground for time scales of a decade or more and is delivered to the stream as baseflow and seepage flow. The decomposition of the flow sources also shows how the transfer of elements via groundwater is distributed between a fast component (one year for the seepage flow) and a much slower component (several tens of years for the baseflow), which indicates that changes in agricultural practices or land use will both have a rapid impact (ca. 1 year) and will also have impacts over the long term (tens of years). This complexity should be accounted for in watershed management.

Acknowledgments

We acknowledge the Agence Nationale de la Recherche (ANR) for its funding through the "Investissements d'avenir" program under the project CZTOP (n°ANR-17-MPGA-0009). The model hs1D is available on github `github.com/jmarcais/hs1D_beta` (Marçais, 2021). Data used for this study are available at `doi.org/10.15454/UYXOEB`. We thank Aurélie Guillou, Virginie Vergnaud and Thierry Labasque for the chemical analysis in the Condate-Eau (Rennes 1) analytical platform and the help on the field. We thank Ciaran Harman for insightful discussions and Sylvain Kuppel for reviewing a former version of this manuscript.

This article is protected by copyright. All rights reserved.

Appendix A Separation of lateral and vertical velocity term

Considering that the water is incompressible, we have the relation $\nabla \mathbf{v} = \frac{dv_x}{dx} + \frac{dv_y}{dy} + \frac{dv_z}{dz} = 0$ (Strack, 1984; Pollock, 1988; Harman, 2019). Deriving v_x with respect to x (cf. equation 2), we get:

$$\begin{aligned} \frac{dv_x}{dx} &= \frac{\phi_d}{\phi_{tot}} v_x \left(\frac{1}{Q}\frac{dQ}{dx} - \frac{1}{S}\frac{dS}{dx} \right) \\ &= \frac{\phi_d}{\phi_{tot}} v_x \left(\frac{1}{Q}\frac{dQ}{dx} - \frac{1}{h}\frac{dh}{dx} - \frac{1}{\omega}\frac{d\omega}{dx} \right) \end{aligned} \tag{7}$$

Applying symmetry principles (Curie, 1894), we can attribute the part of this quantity invariant to z to the quantity $\frac{dv_y}{dy}$:

$$\frac{dv_y}{dy} = \frac{\phi_d}{\phi_{tot}} \frac{1}{\omega}\frac{d\omega}{dx} v_x \tag{8}$$

This enables derivation of v_z:

$$\begin{aligned} \frac{dv_z}{dz} &= -\frac{dv_x}{dx} - \frac{dv_y}{dy} \\ &= -\frac{\phi_d}{\phi_{tot}} \left(\frac{d}{dx}\left(\frac{Q}{S}\right) + \frac{1}{\omega}\frac{d\omega}{dx}\frac{Q}{S} \right) \end{aligned} \tag{9}$$

Hence, as $\frac{dv_z}{dz}$ does not depend on z:

$$v_z = z\frac{dv_z}{dz} = -z\frac{\phi_d}{\phi_{tot}} \left(\frac{d}{dx}\left(\frac{Q}{S}\right) + \frac{1}{w}\frac{dw}{dx}\frac{Q}{S} \right) \tag{10}$$

2D flow lines $\mathbf{x}(t) = (x(t), z(t))$ derive from the Lagrangian definition of velocity where the temporal derivative of the trajectory $\mathbf{x}(t)$ is linked to the velocity field: $\frac{d\mathbf{x}}{dt} = \mathbf{v}(\mathbf{x}(t)) = (v_x(x(t), z(t), t), v_z(x(t), z(t), t))$.

References

Ameli, A. A., Beven, K., Erlandsson, M., Creed, I. F., McDonnell, J. J., & Bishop, K. (2017). Primary weathering rates, water transit times, and concentration-discharge relations: A theoretical analysis for the critical zone. *Water Resour. Res.*, *53*(1), 942–960. doi: 10.1002/2016WR019448

Anderson, R. S., Rajaram, H., & Anderson, S. P. (2019). Climate driven coevolution of weathering profiles and hillslope topography generates dramatic differences in critical zone architecture. *Hydrol. Process.*, *33*(1), 4–19. doi: 10.1002/hyp.13307

Anderson, S. P., Dietrich, W. E., Montgomery, D. R., Torres, R., Conrad, M. E., & Loague, K. (1997). Subsurface flow paths in a steep, unchanneled catchment. *Water Resour. Res.*, *33*(12), 2637–2653. doi: 10.1029/97WR02595

Aquilina, L., Vergnaud-Ayraud, V., Labasque, T., Bour, O., Molénat, J., Ruiz, L., ... Longuevergne, L. (2012). Nitrate dynamics in agricultural catchments deduced from groundwater dating and long-term nitrate monitoring in surface-

This article is protected by copyright. All rights reserved.

Accepted Article

and groundwaters. *Science of The Total Environment*, *435–436*, 167–178. doi: 10.1016/j.scitotenv.2012.06.028

Ayraud, V., Aquilina, L., Labasque, T., Pauwels, H., Molenat, J., Pierson-Wickmann, A.-C., ... Davy, P. (2008). Compartmentalization of physical and chemical properties in hard-rock aquifers deduced from chemical and groundwater age analyses. *Applied Geochemistry*, *23*(9), 2686–2707. doi: 10.1016/j.apgeochem.2008.06.001

Benettin, P., Bailey, S. W., Rinaldo, A., Likens, G. E., McGuire, K. J., & Botter, G. (2017). Young runoff fractions control streamwater age and solute concentration dynamics. *Hydrol. Process.*, *31*(16), 2982–2986. doi: 10.1002/hyp.11243

Benettin, P., & Bertuzzo, E. (2018). Tran-SAS v1.0: A numerical model to compute catchment-scale hydrologic transport using StorAge Selection functions. *Geosci. Model Dev.*, *11*(4), 1627–1639. doi: 10.5194/gmd-11-1627-2018

Benettin, P., Scott W. Bailey, Campbell, J. L., Green, M., Rinaldo, A., Likens Gene E., ... Botter Gianluca (2015). Linking water age and solute dynamics in streamflow at the Hubbard Brook Experimental Forest, NH, USA. *Water Resources Research*, *51*(11), 9256–9272. doi: 10.1002/2015WR017552

Benettin, P., Soulsby, C., Birkel, C., Tetzlaff, D., Botter, G., & Rinaldo, A. (2017). Using SAS functions and high-resolution isotope data to unravel travel time distributions in headwater catchments. *Water Resour. Res.*, *53*(3), 1864–1878. doi: 10.1002/2016WR020117

Berghuijs, W. R., & Kirchner, J. W. (2017). The relationship between contrasting ages of groundwater and streamflow: Connecting Storage and Streamflow Ages. *Geophys. Res. Lett.*, *44*(17), 8925–8935. doi: 10.1002/2017GL074962

Blume, T., & van Meerveld, H. I. (2015). From hillslope to stream: Methods to investigate subsurface connectivity: Methods to investigate subsurface connectivity. *WIREs Water*, *2*(3), 177–198. doi: 10.1002/wat2.1071

Boone, A., Samuelsson, P., Gollvik, S., Napoly, A., Jarlan, L., Brun, E., & Decharme, B. (2017). The interactions between soil–biosphere–atmosphere land surface model with a multi-energy balance (ISBA-MEB) option in SURFEXv8 – Part 1: Model description. *Geosci. Model Dev.*, *10*(2), 843–872. doi: 10.5194/gmd-10-843-2017

Botter, M., Li, L., Hartmann, J., Burlando, P., & Fatichi, S. (2020). Depth of Solute Generation Is a Dominant Control on Concentration-Discharge Relations. *Water Resour. Res.*, *56*(8), e2019WR026695. doi: 10.1029/2019WR026695

Boussinesq, J. (1877). *Essai sur la théorie des eaux courantes.* Imprimerie Nationale.

Brantley, S. L., McDowell, W. H., Dietrich, W. E., White, T. S., Kumar, P., Anderson, S. P., ... Gaillardet, J. (2017). Designing a network of critical zone observatories to explore the living skin of the terrestrial Earth. *Earth Surf. Dyn.*, *5*(4), 841–860. doi: 10.5194/esurf-5-841-2017

Brutsaert, W. B., & Nieber, J. L. (1977). Regionalized drought flow hydrographs from a mature glaciated plateau. *Water Resour. Res.*, *13*(3), 637–643. doi: 10.1029/WR013i003p00637

Camporese, M., Paniconi, C., Putti, M., & Orlandini, S. (2010). Surface-subsurface flow modeling with path-based runoff routing, boundary condition-based coupling, and assimilation of multisource observation data. *Water Resour. Res.*, *46*(2), W02512. doi: 10.1029/2008WR007536

This article is protected by copyright. All rights reserved.

Accepted Article

Carrera, J., Sánchez-Vila, X., Benet, I., Medina, A., Galarza, G., & Guimerà, J. (1998). On matrix diffusion: Formulations, solution methods and qualitative effects. *Hydrogeology Journal*, *6*(1), 178–190. doi: 10.1007/s100400050143

Cenki-Tok, B., Chabaux, F., Lemarchand, D., Schmitt, A. D., Pierret, M. C., Viville, D., ... Stille, P. (2009). The impact of water–rock interaction and vegetation on calcium isotope fractionation in soil- and stream waters of a small, forested catchment (the Strengbach case). *Geochimica et Cosmochimica Acta*, *73*(8), 2215–2228. doi: 10.1016/j.gca.2009.01.023

Chen, N., Valdes, D., Marlin, C., Blanchoud, H., Guerin, R., Rouelle, M., & Ribstein, P. (2019). Water, nitrate and atrazine transfer through the unsaturated zone of the Chalk aquifer in northern France. *Science of The Total Environment*, *652*, 927–938. doi: 10.1016/j.scitotenv.2018.10.286

Chesnaux, R., Molson, J., & Chapuis, R. (2005). An Analytical Solution for Ground Water Transit Time through Unconfined Aquifers. *Ground Water*, *43*(4), 511–517. doi: 10.1111/j.1745-6584.2005.0056.x

Clément, J.-C., Holmes, R. M., Peterson, B. J., & Pinay, G. (2003). Isotopic investigation of denitrification in a riparian ecosystem in western France. *J. Appl. Ecol.*, *40*(6), 1035–1048. Retrieved from `http://onlinelibrary.wiley.com/doi/10.1111/j.1365-2664.2003.00854.x/full`

Conan, C., Bouraoui, F., Turpin, N., de Marsily, G., & Bidoglio, G. (2003). Modeling Flow and Nitrate Fate at Catchment Scale in Brittany (France). *J. Environ. Qual.*, *32*(6), 2026–2032. doi: 10.2134/jeq2003.2026

Curie, P. (1894). Sur la symétrie dans les phénomènes physiques, symétrie d'un champ électrique et d'un champ magnétique. *J. Phys. Theor. Appl.*, *3*(1), 393–415. doi: 10.1051/jphystap:018940030039300

Danckwerts, P. V. (1953). Continuous flow systems: Distribution of residence times. *Chemical Engineering Science*, *2*(1), 1–13. doi: 10.1016/0009-2509(53)80001-1

de Dreuzy, J.-R., Beaudoin, A., & Erhel, J. (2007). Asymptotic dispersion in 2D heterogeneous porous media determined by parallel numerical simulations. *Water Resour. Res.*, *43*(10). doi: 10.1029/2006WR005394

de Dreuzy, J.-R., Carrera, J., Dentz, M., & Borgne, T. L. (2012). Asymptotic dispersion for two-dimensional highly heterogeneous permeability fields under temporally fluctuating flow. *Water Resour. Res.*, *48*(1). doi: 10.1029/2011WR011129

Dunkle, S. A., Plummer, L. N., Busenberg, E., Phillips, P. J., Denver, J. M., Hamilton, P. A., ... Coplen, T. B. (1993). Chlorofluorocarbons (CCl3F and CCl2F2) as dating tools and hydrologic tracers in shallow groundwater of the Delmarva Peninsula, Atlantic Coastal Plain, United States. *Water Resour. Res.*, *29*(12), 3837–3860. doi: 10.1029/93WR02073

Dupuit, J. (1863). *Études théoriques et pratiques sur le mouvement des eaux dans les canaux découverts et à travers les terrains perméables : avec des considérations relatives au régime des grandes eaux, au débouché à leur donner, et à la marche des alluvions dans les rivières à fond mobile (2e édition revue et considérablement augmentée) / par J. Dupuit...* Retrieved from `https://gallica.bnf.fr/ark:/12148/bpt6k62096061`

Ehrhardt, S., Kumar, R., Fleckenstein, J. H., Attinger, S., & Musolff, A. (2019). Trajectories of nitrate input and output in three nested catchments along

This article is protected by copyright. All rights reserved.

Accepted Article

a land use gradient. *Hydrol. Earth Syst. Sci.*, *23*(9), 3503–3524. doi: 10.5194/hess-23-3503-2019

Engdahl, N. B., & Maxwell, R. M. (2014). Approximating groundwater age distributions using simple streamtube models and multiple tracers. *Advances in Water Resources*, *66*, 19–31. doi: 10.1016/j.advwatres.2014.02.001

Engesgaard, P., Højberg, A. L., Hinsby, K., Jensen, K. H., Laier, T., Larsen, F., ... Plummer, L. N. (2004). Transport and Time Lag of Chlorofluorocarbon Gases in the Unsaturated Zone, Rabis Creek, Denmark. *Vadose Zone J.*, *3*(4), 1249–1261. doi: 10.2136/vzj2004.1249

Fan, Y., & Bras, R. L. (1998). Analytical solutions to hillslope subsurface storm flow and saturation overland flow. *Water Resour. Res.*, *34*(4), 921–927. doi: 10.1029/97WR03516

Fang, Z., Carroll, R. W. H., Schumer, R., Harman, C., Wilusz, D., & Williams, K. H. (2019). Streamflow partitioning and transit time distribution in snow-dominated basins as a function of climate. *Journal of Hydrology*, *570*, 726–738. doi: 10.1016/j.jhydrol.2019.01.029

Farr, T. G., Rosen, P. A., Caro, E., Crippen, R., Duren, R., Hensley, S., ... Alsdorf, D. (2007). The Shuttle Radar Topography Mission. *Rev. Geophys.*, *45*(2), RG2004. doi: 10.1029/2005RG000183

Fatichi, S., Vivoni, E. R., Ogden, F. L., Ivanov, V. Y., Mirus, B., Gochis, D., ... Tarboton, D. (2016). An overview of current applications, challenges, and future trends in distributed process-based models in hydrology. *Journal of Hydrology*, *537*, 45–60. doi: 10.1016/j.jhydrol.2016.03.026

Ferguson, G., Cuthbert, M., Befus, K. M., Gleeson, T., & McIntosh, J. C. (2020). *The groundwater age-sustainability myth* (Preprint). EarthArXiv. doi: 10.31223/osf.io/gq2m3

Fernandez, N. M., Perez-Fodich, A., Derry, L. A., & Druhan, J. L. (2021). A first look at Ge/Si partitioning during amorphous silica precipitation: Implications for Ge/Si as a tracer of fluid-silicate interactions. *Geochimica et Cosmochimica Acta*, *297*, 158–178. doi: 10.1016/j.gca.2021.01.007

Freer, J., McDonnell, J. J., Beven, K. J., Peters, N. E., Burns, D. A., Hooper, R. P., ... Kendall, C. (2002). The role of bedrock topography on subsurface storm flow. *Water Resour. Res.*, *38*(12), 1269. doi: 10.1029/2001WR000872

von Freyberg, J., Studer, B., Rinderer, M., & Kirchner, J. W. (2018). Studying catchment storm response using event and pre-event water volumes as fractions of precipitation rather than discharge. *Hydrol. Earth Syst. Sci. Discuss.*, 1–34. doi: 10.5194/hess-2018-401

Frisbee, M. D., Wilson, J. L., Gomez-Velez, J. D., Phillips, F. M., & Campbell, A. R. (2013). Are we missing the tail (and the tale) of residence time distributions in watersheds? *Geophys. Res. Lett.*, *40*(17), 4633–4637. doi: 10.1002/grl.50895

Gabrielli, C. P., & McDonnell, J. J. (2020). Modifying the Jackson index to quantify the relationship between geology, landscape structure, and water transit time in steep wet headwaters. *Hydrol. Process.*, *34*(9), 2139–2150. doi: 10.1002/hyp.13700

Gabrielli, C. P., Morgenstern, U., Stewart, M. K., & McDonnell, J. J. (2018). Contrasting Groundwater and Streamflow Ages at the Maimai Watershed. *Water Resour. Res.*, *54*(6), 3937–3957. doi: 10.1029/2017WR021825

This article is protected by copyright. All rights reserved.

Accepted Article

Gardner, W. P., Harrington, G. A., Solomon, D. K., & Cook, P. G. (2011). Using terrigenic 4He to identify and quantify regional groundwater discharge to streams. *Water Resour. Res.*, *47*(6). doi: 10.1029/2010WR010276

Gauvain, A., Leray, S., Marçais, J., Roques, C., Vautier, C., Gresselin, F., ... de Dreuzy, J.-R. (2021). Geomorphological Controls on Groundwater Transit Times: A Synthetic Analysis at the Hillslope Scale. *Water Resour. Res.*, *57*(7), e2020WR029463. doi: 10.1029/2020WR029463

Gelhar, L. W., & Axness, C. L. (1983). Three-dimensional stochastic analysis of macrodispersion in aquifers. *Water Resour. Res.*, *19*(1), 161–180. doi: 10.1029/WR019i001p00161

Gelhar, L. W., Welty, C., & Rehfeldt, K. R. (1992). A critical review of data on field-scale dispersion in aquifers. *Water Resour. Res.*, *28*(7), 1955–1974. doi: 10.1029/92WR00607

Gleeson, T., & Manning, A. H. (2008). Regional groundwater flow in mountainous terrain: Three-dimensional simulations of topographic and hydrogeologic controls. *Water Resour. Res.*, *44*(10). doi: 10.1029/2008WR006848

Green, C. T., Liao, L., Nolan, B. T., Juckem, P. F., Shope, C. L., Tesoriero, A. J., & Jurgens, B. C. (2018). Regional Variability of Nitrate Fluxes in the Unsaturated Zone and Groundwater, Wisconsin, USA. *Water Resour. Res.*, *54*(1), 301–322. doi: 10.1002/2017WR022012

Grimaldi, C., Thomas, Z., Fossey, M., Fauvel, Y., & Merot, P. (2009). High chloride concentrations in the soil and groundwater under an oak hedge in the West of France: An indicator of evapotranspiration and water movement. *Hydrol. Process.*, *23*(13), 1865–1873. doi: 10.1002/hyp.7316

Guérin, A., Devauchelle, O., Robert, V., Kitou, T., Dessert, C., Quiquerez, A., ... Lajeunesse, E. (2019). Stream-Discharge Surges Generated by Groundwater Flow. *Geophys. Res. Lett.*, *46*(13), 7447–7455. doi: 10.1029/2019GL082291

Guillaumot, L., Marçais, J., Vautier, C., Guillou, A., Vergnaud, V., Bouchez, C., ... Aquilina, L. (2021). A hillslope-scale aquifer-model to determine past agricultural legacy and future nitrate concentrations in rivers. *Science of The Total Environment*, 149216. doi: 10.1016/j.scitotenv.2021.149216

Gupta, H. V., Kling, H., Yilmaz, K. K., & Martinez, G. F. (2009). Decomposition of the mean squared error and NSE performance criteria: Implications for improving hydrological modelling. *Journal of Hydrology*, *377*(1), 80–91. doi: 10.1016/j.jhydrol.2009.08.003

Gustard, A., Bullock, A., & Dixon, J. M. (1992). *Low flow estimation in the United Kingdom*. Institute of Hydrology.

Haggerty, R., & Gorelick, S. M. (1995). Multiple-Rate Mass Transfer for Modeling Diffusion and Surface Reactions in Media with Pore-Scale Heterogeneity. *Water Resour. Res.*, *31*(10), 2383–2400. doi: 10.1029/95WR10583

Haitjema, H. M. (1995). On the residence time distribution in idealized groundwatersheds. *Journal of Hydrology*, *172*(1), 127–146. doi: 10.1016/0022-1694(95)02732-5

Haitjema, H. M., & Mitchell-Bruker, S. (2005). Are Water Tables a Subdued Replica of the Topography? *Groundwater*, *43*(6), 781–786. doi: 10.1111/j.1745-6584.2005.00090.x

Harman, C. J. (2014). Time-variable transit time distributions and transport: Theory and application to storage-dependent transport of chloride in a watershed.

This article is protected by copyright. All rights reserved.

Accepted Article

Water Resources Research, *51*(1), 1–30. doi: 10.1002/2014WR015707

Harman, C. J. (2019). Age-Ranked Storage-Discharge Relations: A Unified Description of Spatially Lumped Flow and Water Age in Hydrologic Systems. *Water Resour. Res.*, *55*(8), 7143–7165. doi: 10.1029/2017WR022304

Harman, C. J., Rao, P. S. C., Basu, N. B., McGrath, G. S., Kumar, P., & Sivapalan, M. (2011). Climate, soil, and vegetation controls on the temporal variability of vadose zone transport. *Water Resour. Res.*, *47*(10). doi: 10.1029/2010WR010194

Heidbüchel, I., Troch, P. A., & Lyon, S. W. (2013). Separating physical and meteorological controls of variable transit times in zero-order catchments. *Water Resour. Res.*, *49*(11), 7644–7657. doi: 10.1002/2012WR013149

Heidbüchel, I., Troch, P. A., Lyon, S. W., & Weiler, M. (2012). The master transit time distribution of variable flow systems. *Water Resour. Res.*, *48*(6), W06520. doi: 10.1029/2011WR011293

Heidbüchel, I., Yang, J., Musolff, A., Troch, P., Ferré, T., & Fleckenstein, J. H. (2020). On the shape of forward transit time distributions in low-order catchments. *Hydrol. Earth Syst. Sci.*, *24*(6), 2895–2920. doi: 10.5194/hess-24-2895-2020

Hunt, B. (1998). Contaminant Source Solutions with Scale-Dependent Dispersivities. *Journal of Hydrologic Engineering*, *3*(4), 268–275. doi: 10.1061/(ASCE)1084-0699(1998)3:4(268)

Jackson, C. R., Bitew, M., & Du, E. (2014). When interflow also percolates: Downslope travel distances and hillslope process zones. *Hydrol. Process.*, *28*(7), 3195–3200. doi: 10.1002/hyp.10158

Jasechko, S., Kirchner, J. W., Welker, J. M., & McDonnell, J. J. (2016). Substantial proportion of global streamflow less than three months old. *Nat. Geosci.*, *9*(2), 126–129. doi: 10.1038/ngeo2636

Kaandorp, V. P., Louw, P. G. B., Velde, Y., & Broers, H. P. (2018). Transient Groundwater Travel Time Distributions and Age-Ranked Storage-Discharge Relationships of Three Lowland Catchments. *Water Resour. Res.*, *54*(7), 4519–4536. doi: 10.1029/2017WR022461

Kazemi, G. A., Lehr, J. H., & Perrochet, P. (2006). *Groundwater Age*. John Wiley & Sons.

Kirchner, J. W. (2016). Aggregation in environmental systems - Part 1: Seasonal tracer cycles quantify young water fractions, but not mean transit times, in spatially heterogeneous catchments. *Hydrol. Earth Syst. Sci.*, *20*(1), 279–297. doi: 10.5194/hess-20-279-2016

Kirchner, J. W., Feng, X., & Neal, C. (2000). Fractal stream chemistry and its implications for contaminant transport in catchments. *Nature*, *403*(6769), 524. doi: 10.1038/35000537

Kirchner, J. W., Feng, X., & Neal, C. (2001). Catchment-scale advection and dispersion as a mechanism for fractal scaling in stream tracer concentrations. *Journal of Hydrology*, *254*(1–4), 82–101. doi: 10.1016/S0022-1694(01)00487-5

Klaus, J., & Jackson, C. R. (2018). Interflow Is Not Binary: A Continuous Shallow Perched Layer Does Not Imply Continuous Connectivity. *Water Resour. Res.*, *54*(9), 5921–5932. doi: 10.1029/2018WR022920

Kolbe, T., de Dreuzy, J.-R., Abbott, B. W., Aquilina, L., Babey, T., Green, C. T., ... Pinay, G. (2019). Stratification of reactivity determines nitrate removal in

This article is protected by copyright. All rights reserved.

Accepted Article

groundwater. *PNAS*, 201816892. doi: 10.1073/pnas.1816892116

Kolbe, T., Marçais, J., de Dreuzy, J.-R., Labasque, T., & Bishop, K. (2020). Lagged rejuvenation of groundwater indicates internal flow structures and hydrological connectivity. *Hydrol. Process.*, *34*(10), 2176–2189. doi: 10.1002/hyp.13753

Kolbe, T., Marçais, J., Thomas, Z., Abbott, B. W., de Dreuzy, J.-R., Rousseau-Gueutin, P., ... Pinay, G. (2016). Coupling 3D groundwater modeling with CFC-based age dating to classify local groundwater circulation in an unconfined crystalline aquifer. *Journal of Hydrology*, *543*, 31–46. doi: 10.1016/j.jhydrol.2016.05.020

Kollet, S. J., & Maxwell, R. M. (2006). Integrated surface–groundwater flow modeling: A free-surface overland flow boundary condition in a parallel groundwater flow model. *Advances in Water Resources*, *29*(7), 945–958. doi: 10.1016/j.advwatres.2005.08.006

Kosugi, K., Katsura, S., Mizuyama, T., Okunaka, S., & Mizutani, T. (2008). Anomalous behavior of soil mantle groundwater demonstrates the major effects of bedrock groundwater on surface hydrological processes. *Water Resour. Res.*, *44*(1). doi: 10.1029/2006WR005859

Kuppel, S., Tetzlaff, D., Maneta, M. P., & Soulsby, C. (2020). Critical Zone Storage Controls on the Water Ages of Ecohydrological Outputs. *Geophys. Res. Lett.*, *47*(16), e2020GL088897. doi: 10.1029/2020GL088897

Kurtz, A. C., Lugolobi, F., & Salvucci, G. (2011). Germanium-silicon as a flow path tracer: Application to the Rio Icacos watershed. *Water Resources Research*, *47*(6). doi: 10.1029/2010WR009853

Labasque, T., Aquilina, L., Vergnaud, V., & Barbecot, F. (2014). Inter-laboratory comparison of the analyses of sulphur hexafluoride (SF6) and three chlorofluorocarbons (CFC-11, -12 and -113) in groundwater and an air standard. *Applied Geochemistry*, *50*, 118–129. doi: 10.1016/j.apgeochem.2014.03.009

Le Borgne, T., Bour, O., Paillet, F. L., & Caudal, J. P. (2006). Assessment of preferential flow path connectivity and hydraulic properties at single-borehole and cross-borehole scales in a fractured aquifer. *Journal of Hydrology*, *328*(1–2), 347–359. doi: 10.1016/j.jhydrol.2005.12.029

Legchenko, A., Baltassat, J.-M., Bobachev, A., Martin, C., Robain, H., & Vouillamoz, J.-M. (2004). Magnetic Resonance Sounding Applied to Aquifer Characterization. *Groundwater*, *42*(3), 363–373. doi: 10.1111/j.1745-6584.2004.tb02684.x

Legout, C., Molenat, J., Aquilina, L., Gascuel-Odoux, C., Faucheux, M., Fauvel, Y., & Bariac, T. (2007). Solute transfer in the unsaturated zone-groundwater continuum of a headwater catchment. *Journal of Hydrology*, *332*(3), 427–441. doi: 10.1016/j.jhydrol.2006.07.017

Le Moigne, P., Besson, F., Martin, E., Boé, J., Boone, A., Decharme, B., ... Rousset-Regimbeau, F. (2020). The latest improvements with SURFEX v8.0 of the Safran–Isba–Modcou hydrometeorological model for France. *Geosci. Model Dev.*, *13*(9), 3925–3946. doi: 10.5194/gmd-13-3925-2020

Leray, S., de Dreuzy, J. R., Bour, O., Labasque, T., & Aquilina, L. (2012). Contribution of age data to the characterization of complex aquifers. *Journal of Hydrology*, *464–465*, 54–68. doi: 10.1016/j.jhydrol.2012.06.052

Li, L., Maher, K., Navarre-Sitchler, A., Druhan, J., Meile, C., Lawrence, C., ... Beisman, J. (2017). Expanding the role of reactive transport mod-

This article is protected by copyright. All rights reserved.

Accepted Article

els in critical zone processes. *Earth-Science Reviews*, *165*, 280–301. doi: 10.1016/j.earscirev.2016.09.001

Loritz, R., Hassler, S. K., Jackisch, C., Allroggen, N., van Schaik, L., Wienhöfer, J., & Zehe, E. (2017). Picturing and modeling catchments by representative hillslopes. *Hydrol. Earth Syst. Sci.*, *21*(2), 1225–1249. doi: 10.5194/hess-21-1225-2017

L'vovich, M. I. (1979). *World Water Resources and Their Future.* Washington, D. C.: American Geophysical Union. doi: 10.1029/SP013

Lyne, V., & Hollick, M. (1979). Stochastic time-variable rainfall-runoff modelling. In *Institute of Engineers Australia National Conference* (Vol. 1979, pp. 89–93). Institute of Engineers Australia Barton, Australia.

Maher, K. (2010). The dependence of chemical weathering rates on fluid residence time. *Earth and Planetary Science Letters*, *294*(1–2), 101–110. doi: 10.1016/j.epsl.2010.03.010

Maher, K. (2011). The role of fluid residence time and topographic scales in determining chemical fluxes from landscapes. *Earth and Planetary Science Letters*, *312*(1), 48–58. doi: 10.1016/j.epsl.2011.09.040

Maher, K., & Druhan, J. (2014). Relationships between the Transit Time of Water and the Fluxes of Weathered Elements through the Critical Zone. *Procedia Earth and Planetary Science*, *10*, 16–22. doi: 10.1016/j.proeps.2014.08.004

Małoszewski, P., & Zuber, A. (1982). Determining the turnover time of groundwater systems with the aid of environmental tracers: 1. Models and their applicability. *Journal of Hydrology*, *57*(3), 207–231. doi: 10.1016/0022-1694(82)90147-0

Manning, A. H., Clark, J. F., Diaz, S. H., Rademacher, L. K., Earman, S., & Niel Plummer, L. (2012). Evolution of groundwater age in a mountain watershed over a period of thirteen years. *Journal of Hydrology*, *460–461*, 13–28. doi: 10.1016/j.jhydrol.2012.06.030

Marçais, J. (2021). *Jmarcais/hs1D_beta: hs1D flux and transport.* Zenodo. doi: 10.5281/zenodo.5234909

Marçais, J., de Dreuzy, J. R., & Erhel, J. (2017). Dynamic coupling of subsurface and seepage flows solved within a regularized partition formulation. *Advances in Water Resources*, *109*(Supplement C), 94–105. doi: 10.1016/j.advwatres.2017.09.008

Marçais, J., de Dreuzy, J. R., Ginn, T. R., Rousseau-Gueutin, P., & Leray, S. (2015). Inferring transit time distributions from atmospheric tracer data: Assessment of the predictive capacities of Lumped Parameter Models on a 3D crystalline aquifer model. *Journal of Hydrology*, *525*, 619–631. doi: 10.1016/j.jhydrol.2015.03.055

Marçais, J., Gauvain, A., Labasque, T., Abbott, B. W., Pinay, G., Aquilina, L., ... de Dreuzy, J.-R. (2018). Dating groundwater with dissolved silica and CFC concentrations in crystalline aquifers. *Science of The Total Environment*, *636*, 260–272. doi: 10.1016/j.scitotenv.2018.04.196

de Marsily, G. (1986). *Quantitative hydrogeology: Groundwater hydrology for engineers.* Academic Press.

Martin, C., Molénat, J., Gascuel-Odoux, C., Vouillamoz, J. M., Robain, H., Ruiz, L., ... Aquilina, L. (2006). Modelling the effect of physical and chemical characteristics of shallow aquifers on water and nitrate transport in small agricultural catchments. *Journal of Hydrology*, *326*(1–4), 25–42. doi:

This article is protected by copyright. All rights reserved.

Accepted Article

10.1016/j.jhydrol.2005.10.040

Maxwell, R. M., Condon, L. E., Kollet, S. J., Maher, K., Haggerty, R., & Forrester, M. M. (2016). The imprint of climate and geology on the residence times of groundwater. *Geophys. Res. Lett.*, 2015GL066916. doi: 10.1002/2015GL066916

McDonnell, J. J. (2017). *Beyond the water balance* [Comments and Opinion]. doi: 10.1038/ngeo2964

McDonnell, J. J., & Beven, K. (2014). Debates—The future of hydrological sciences: A (common) path forward? a call to action aimed at understanding velocities, celerities and residence time distributions of the headwater hydrograph. *Water Resour. Res.*, *50*(6), 5342–5350. doi: 10.1002/2013WR015141

Molenat, J. (1999). *Rôle de la nappe sur les transferts d'eau et de nitrate dans un bassin versant agricole : étude expérimentale et modélisation* (Doctoral dissertation, Rennes 1). Retrieved from `http://www.theses.fr/1999REN1A004`

de Montety, V., Aquilina, L., Labasque, T., Chatton, E., Fovet, O., Ruiz, L., ... de Dreuzy, J. R. (2018). Recharge processes and vertical transfer investigated through long-term monitoring of dissolved gases in shallow groundwater. *Journal of Hydrology*, *560*, 275–288. doi: 10.1016/j.jhydrol.2018.02.077

Montgomery, D. R., Dietrich, W. E., Torres, R., Anderson, S. P., Heffner, J. T., & Loague, K. (1997). Hydrologic response of a steep, unchanneled valley to natural and applied rainfall. *Water Resour. Res.*, *33*(1), 91–109. doi: 10.1029/96WR02985

Morgenstern, U., Stewart, M. K., & Stenger, R. (2010). Dating of streamwater using tritium in a post nuclear bomb pulse world: Continuous variation of mean transit time with streamflow. *Hydrol. Earth Syst. Sci.*, *14*(11), 2289–2301. doi: 10.5194/hess-14-2289-2010

Mougin, B., Allier, D., Blanchin, R., Carn, A., Courtois, N., Gateau, C., ... Wyns, R. (2008). *SILURES Bretagne - Rapport final - Année 5* (Tech. Rep. No. RP-56457-FR). Retrieved from `http://infoterre.brgm.fr/rapports/RP-56457-FR.pdf`

Mougin, B., Carn, A., Thomas, E., & Jégou, J.-P. (2002). *SILURES Bretagne Etat d'avancement de l'année 1* (Tech. Rep. No. RP-51481-FR). Retrieved from `http://infoterre.brgm.fr/rapports/RP-51481-FR.pdf`

Mougin, B., Thomas, E., Mathieu, F., Baltassat, J.-M., Schroetter, J.-M., Blanchin, R., ... Lucassou, F. (2015). *Calcul des volumes d'eau souterraine sur 12 bassins versants bretons en zone de socle et apports sur les temps moyens de résidence des eaux souterraines.* Retrieved from `https://hal-brgm.archives-ouvertes.fr/hal-01180210`

Mougin, B., Thomas, E., Wyns, R., Blanchin, R., & Mathieu, F. (2004). *Qualité des eaux en Bretagne - Ruissellement - Infiltration - Temps de réponse. Bassins versants : Le Yar (Côtes d'Armor), l'Horn (Finistère), et du Coët-Dan (Morbihan)* (Tech. Rep. No. RP-52731-FR). BRGM. Retrieved from `http://infoterre.brgm.fr/rapports//RP-52731-FR.pdf`

Musy, A., & Higy, C. (2004). *Hydrologie: Une science de la nature.* PPUR presses polytechniques.

Nguyen, T. V., Kumar, R., Lutz, S. R., Musolff, A., Yang, J., & Fleckenstein, J. H. (2021). Modeling Nitrate Export From a Mesoscale Catchment Using StorAge Selection Functions. *Water Resour. Res.*, *57*(2), e2020WR028490. doi:

This article is protected by copyright. All rights reserved.

Accepted Article

10.1029/2020WR028490

Paniconi, C., & Putti, M. (2015). Physically based modeling in catchment hydrology at 50: Survey and outlook: SURVEY OF PHYSICALLY BASED MODELING IN CATCHMENT HYDROLOGY. *Water Resour. Res.*, *51*(9), 7090–7129. doi: 10.1002/2015WR017780

Paniconi, C., Troch, P. A., van Loon, E. E., & Hilberts, A. G. J. (2003). Hillslope-storage Boussinesq model for subsurface flow and variable source areas along complex hillslopes: 2. Intercomparison with a three-dimensional Richards equation model. *Water Resour. Res.*, *39*(11), 1317. doi: 10.1029/2002WR001730

Peters, N. E., Burns, D. A., & Aulenbach, B. T. (2014). Evaluation of High-Frequency Mean Streamwater Transit-Time Estimates Using Groundwater Age and Dissolved Silica Concentrations in a Small Forested Watershed. *Aquat Geochem*, *20*(2-3), 183–202. doi: 10.1007/s10498-013-9207-6

Pfankuch, H. (1963). Contribution à l'étude des déplacements de fluides miscibles dans un milieu poreux. *Rev. Inst. Fr. Pet.*, *18*, 215–270.

Pinay, G., Peiffer, S., Dreuzy, J.-R., Krause, S., Hannah, D. M., Fleckenstein, J. H., ... Hubert-Moy, L. (2015). Upscaling Nitrogen Removal Capacity from Local Hotspots to Low Stream Orders' Drainage Basins. *Ecosystems*, *18*(6), 1101–1120. doi: 10.1007/s10021-015-9878-5

Pollock, D. W. (1988). Semianalytical Computation of Path Lines for Finite-Difference Models. *Ground Water*, *26*(6), 743–750. doi: 10.1111/j.1745-6584.1988.tb00425.x

Putti, M., & Paniconi, C. (2004). Time step and stability control for a coupled model of surface and subsurface flow. In C. T. Miller & G. F. Pinder (Eds.), *Developments in Water Science* (Vol. 55, pp. 1391–1402). Elsevier. doi: 10.1016/S0167-5648(04)80152-7

Quintana-Seguí, P., Le Moigne, P., Durand, Y., Martin, E., Habets, F., Baillon, M., ... Morel, S. (2008). Analysis of Near-Surface Atmospheric Variables: Validation of the SAFRAN Analysis over France. *J. Appl. Meteor. Climatol.*, *47*(1), 92–107. doi: 10.1175/2007JAMC1636.1

Rademacher, L. K., Clark, J. F., Clow David W., & Hudson G. Bryant. (2005). Old groundwater influence on stream hydrochemistry and catchment response times in a small Sierra Nevada catchment: Sagehen Creek, California. *Water Resources Research*, *41*(2). doi: 10.1029/2003WR002805

Rademacher, L. K., Clark, J. F., Hudson, G. B., Erman, D. C., & Erman, N. A. (2001). Chemical evolution of shallow groundwater as recorded by springs, Sagehen basin; Nevada County, California. *Chemical Geology*, *179*(1), 37–51. doi: 10.1016/S0009-2541(01)00314-X

Reggiani, P., & Schellekens, J. (2003). Modelling of hydrological responses: The representative elementary watershed approach as an alternative blueprint for watershed modelling. *Hydrol. Process.*, *17*(18), 3785–3789. doi: 10.1002/hyp.5167

Reggiani, P., Sivapalan, M., & Majid Hassanizadeh, S. (1998). A unifying framework for watershed thermodynamics: Balance equations for mass, momentum, energy and entropy, and the second law of thermodynamics. *Advances in Water Resources*, *22*(4), 367–398. doi: 10.1016/S0309-1708(98)00012-8

Remondi, F., Botter, M., Burlando, P., & Fatichi, S. (2019). Variability of transit time distributions with climate and topography: A modelling approach. *Jour-*

This article is protected by copyright. All rights reserved.

Accepted Article

nal of Hydrology, *569*, 37–50. doi: 10.1016/j.jhydrol.2018.11.011

Remondi, F., Kirchner, J. W., Burlando, P., & Fatichi, S. (2018). Water Flux Tracking With a Distributed Hydrological Model to Quantify Controls on the Spatiotemporal Variability of Transit Time Distributions. *Water Resour. Res.*, *54*(4), 3081–3099. doi: 10.1002/2017WR021689

Rinaldo, A., Benettin, P., Harman, C. J., Hrachowitz, M., McGuire, K. J., van der Velde, Y., ... Botter, G. (2015). Storage selection functions: A coherent framework for quantifying how catchments store and release water and solutes: ON STORAGE SELECTION FUNCTIONS. *Water Resour. Res.*, *51*(6), 4840–4847. doi: 10.1002/2015WR017273

Rodriguez, N. B., & Klaus, J. (2019). Catchment Travel Times From Composite StorAge Selection Functions Representing the Superposition of Streamflow Generation Processes. *Water Resour. Res.*, *55*(11), 9292–9314. doi: 10.1029/2019WR024973

Rolle, M., Eberhardt, C., Chiogna, G., Cirpka, O. A., & Grathwohl, P. (2009). Enhancement of dilution and transverse reactive mixing in porous media: Experiments and model-based interpretation. *Journal of Contaminant Hydrology*, *110*(3), 130–142. doi: 10.1016/j.jconhyd.2009.10.003

Roques, C., Bour, O., Aquilina, L., Dewandel, B., Leray, S., Schroetter, J., ... Mougin, B. (2014). Hydrological behavior of a deep sub-vertical fault in crystalline basement and relationships with surrounding reservoirs. *Journal of Hydrology*, *509*, 42–54. doi: 10.1016/j.jhydrol.2013.11.023

Scaini, A., Audebert, M., Hissler, C., Fenicia, F., Gourdol, L., Pfister, L., & Beven, K. J. (2017). Velocity and celerity dynamics at plot scale inferred from artificial tracing experiments and time-lapse ERT. *Journal of Hydrology*, *546*, 28–43. doi: 10.1016/j.jhydrol.2016.12.035

Schwanghart, W., & Scherler, D. (2014). Short Communication: TopoToolbox 2 – MATLAB-based software for topographic analysis and modeling in Earth surface sciences. *Earth Surf. Dynam.*, *2*(1), 1–7. doi: 10.5194/esurf-2-1-2014

Schwientek, M., Maloszewski, P., & Einsiedl, F. (2009). Effect of the unsaturated zone thickness on the distribution of water mean transit times in a porous aquifer. *Journal of Hydrology*, *373*(3), 516–526. doi: 10.1016/j.jhydrol.2009.05.015

Shampine, L., Reichelt, M., & Kierzenka, J. (1999). Solving Index-1 DAEs in MATLAB and Simulink. *SIAM Rev.*, *41*(3), 538–552. doi: 10.1137/S003614459933425X

Solder, J. E., Stolp, B. J., Heilweil, V. M., & Susong, D. D. (2016). Characterization of mean transit time at large springs in the Upper Colorado River Basin, USA: A tool for assessing groundwater discharge vulnerability. *Hydrogeol J*, *24*(8), 2017–2033. doi: 10.1007/s10040-016-1440-9

Sprenger, M., Stumpp, C., Weiler, M., Aeschbach, W., Allen, S. T., Benettin, P., ... Werner, C. (2019). The Demographics of Water: A Review of Water Ages in the Critical Zone. *Rev. Geophys.*, *57*(3), 800–834. doi: 10.1029/2018RG000633

Stolp, B. J., Solomon, D. K., Suckow, A., Vitvar, T., Rank, D., Aggarwal, P. K., & Han, L. F. (2010). Age dating base flow at springs and gaining streams using helium-3 and tritium: Fischa-Dagnitz system, southern Vienna Basin, Austria. *Water Resour. Res.*, *46*(7). doi: 10.1029/2009WR008006

This article is protected by copyright. All rights reserved.

Accepted Article

Strack, O. D. L. (1984). Three-Dimensional Streamlines in Dupuit-Forchheimer Models. *Water Resour. Res.*, *20*(7), 812–822. doi: 10.1029/WR020i007p00812

Suckow, A. (2014). The age of groundwater – Definitions, models and why we do not need this term. *Applied Geochemistry*, *50*, 222–230. doi: 10.1016/j.apgeochem.2014.04.016

Therrien, R., & Sudicky, E. A. (1996). Three-dimensional analysis of variably-saturated flow and solute transport in discretely-fractured porous media. *Journal of Contaminant Hydrology*, *23*(1), 1–44. doi: 10.1016/0169-7722(95)00088-7

Troch, P. A., Berne, A., Bogaart, P., Harman, C., Hilberts, A. G. J., Lyon, S. W., ... Verhoest, N. E. C. (2013). The importance of hydraulic groundwater theory in catchment hydrology: The legacy of Wilfried Brutsaert and Jean-Yves Parlange. *Water Resour. Res.*, *49*(9), 5099–5116. doi: 10.1002/wrcr.20407

Troch, P. A., Paniconi, C., & Emiel van Loon, E. (2003). Hillslope-storage Boussinesq model for subsurface flow and variable source areas along complex hillslopes: 1. Formulation and characteristic response. *Water Resour. Res.*, *39*(11), 1316. doi: 10.1029/2002WR001728

Tromp-van Meerveld, H. J., & McDonnell, J. J. (2006). Threshold relations in subsurface stormflow: 2. The fill and spill hypothesis. *Water Resour. Res.*, *42*(2), W02411. doi: 10.1029/2004WR003800

Van Meter, K. J., & Basu, N. B. (2017). Time lags in watershed-scale nutrient transport: An exploration of dominant controls. *Environ. Res. Lett.*, *12*(8), 084017. doi: 10.1088/1748-9326/aa7bf4

Van Meter, K. J., Basu, N. B., Veenstra, J. J., & Burras, C. L. (2016). The nitrogen legacy: Emerging evidence of nitrogen accumulation in anthropogenic landscapes. *Environ. Res. Lett.*, *11*(3), 035014. doi: 10.1088/1748-9326/11/3/035014

Van Meter, K. J., Cappellen, P. V., & Basu, N. B. (2018). Legacy nitrogen may prevent achievement of water quality goals in the Gulf of Mexico. *Science*, *360*(6387), 427–430. doi: 10.1126/science.aar4462

Vannier, O., Braud, I., & Anquetin, S. (2014). Regional estimation of catchment-scale soil properties by means of streamflow recession analysis for use in distributed hydrological models. *Hydrological Processes*, *28*(26), 6276–6291. doi: 10.1002/hyp.10101

Vautier, C., Abhervé, R., Labasque, T., Laverman, A. M., Guillou, A., Chatton, E., ... de Dreuzy, J.-R. (2020). Mapping gas exchanges in headwater streams with membrane inlet mass spectrometry. *Journal of Hydrology*, *581*, 124398. doi: 10.1016/j.jhydrol.2019.124398

van der Velde, Y., de Rooij, G. H., Rozemeijer, J. C., van Geer, F. C., & Broers, H. P. (2010). Nitrate response of a lowland catchment: On the relation between stream concentration and travel time distribution dynamics. *Water Resour. Res.*, *46*(11), W11534. doi: 10.1029/2010WR009105

van Verseveld, W. J., Barnard, H. R., Graham, C. B., McDonnell, J. J., Brooks, J. R., & Weiler, M. (2017). A sprinkling experiment to quantify celerity–velocity differences at the hillslope scale. *Hydrol. Earth Syst. Sci.*, *21*(11), 5891–5910. doi: 10.5194/hess-21-5891-2017

Vidal, J.-P., Martin, E., Franchistéguy, L., Baillon, M., & Soubeyroux, J.-M. (2010). A 50-year high-resolution atmospheric reanalysis over France with the Safran

This article is protected by copyright. All rights reserved.

Accepted Article

system. *Int. J. Climatol.*, *30*(11), 1627–1644. doi: 10.1002/joc.2003

Visser, A., Thaw, M., Deinhart, A., Bibby, R., Safeeq, M., Conklin, M., ... Van der Velde, Y. (2019). Cosmogenic Isotopes Unravel the Hydrochronology and Water Storage Dynamics of the Southern Sierra Critical Zone. *Water Resour. Res.*, *55*(2), 1429–1450. doi: 10.1029/2018WR023665

Vogel, J. C. (1967). Investigation of groundwater flow with radiocarbon. In *Isotopes in hydrology. Proceedings of a symposium.* Retrieved from `http://inis.iaea.org/Search/search.aspx?orig_q=RN:38061071`

White, R. E., Wellings, S. R., & Bell, J. P. (1983). Seasonal variations in nitrate leaching in structured clay soils under mixed land use. *Agricultural Water Management*, *7*(4), 391–410. doi: 10.1016/0378-3774(83)90030-6

Wilson, C. J., & Dietrich, P. (1987). The contribution of bedrock groundwater flow to storm runoff and high pore water pressure development in hollows. *IAHS Publ.*, *165*, 49-59.

Wilusz, D. C., Harman, C. J., & Ball, W. P. (2017). Sensitivity of Catchment Transit Times to Rainfall Variability Under Present and Future Climates. *Water Resour. Res.*, *53*(12), 10231–10256. doi: 10.1002/2017WR020894

Wilusz, D. C., Harman, C. J., Ball, W. P., Maxwell, R. M., & Buda, A. R. (2020). Using Particle Tracking to Understand Flow Paths, Age Distributions, and the Paradoxical Origins of the Inverse Storage Effect in an Experimental Catchment. *Water Resour. Res.*, *56*(4), e2019WR025140. doi: 10.1029/2019WR025140

Wittenberg, H., & Sivapalan, M. (1999). Watershed groundwater balance estimation using streamflow recession analysis and baseflow separation. *Journal of Hydrology*, *219*(1–2), 20–33. doi: 10.1016/S0022-1694(99)00040-2

Yang, J., Heidbüchel, I., Musolff, A., Reinstorf, F., & Fleckenstein, J. H. (2018). Exploring the Dynamics of Transit Times and Subsurface Mixing in a Small Agricultural Catchment. *Water Resources Research*, *0*(0). doi: 10.1002/2017WR021896

Yang, X., Jomaa, S., Zink, M., Fleckenstein, J. H., Borchardt, D., & Rode, M. (2018). A New Fully Distributed Model of Nitrate Transport and Removal at Catchment Scale. *Water Resour. Res.*, *54*(8), 5856–5877. doi: 10.1029/2017WR022380

Zech, A., Attinger, S., Cvetkovic, V., Dagan, G., Dietrich, P., Fiori, A., ... Teutsch, G. (2015). Is unique scaling of aquifer macrodispersivity supported by field data? *Water Resour. Res.*, *51*(9), 7662–7679. doi: 10.1002/2015WR017220

This article is protected by copyright. All rights reserved.

Accepted Article